

VYSOKÉ UČENÍ TECHNICKÉ V BRNĚ

BRNO UNIVERSITY OF TECHNOLOGY

FAKULTA CHEMICKÁ
ÚSTAV CHEMIE MATERIÁLŮ

FACULTY OF CHEMISTRY
INSTITUTE OF MATERIALS SCIENCE

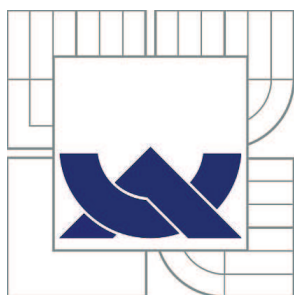
RHEOLOGICAL PROPERTIES OF BIODEGRADABLE
THERMOSENSITIVE COPOLYMERS

DIPLOMOVÁ PRÁCE
MASTER'S THESIS

AUTOR PRÁCE
AUTHOR

Bc. IVANA CHAMRADOVÁ

BRNO 2012



VYSOKÉ UČENÍ TECHNICKÉ V BRNĚ

BRNO UNIVERSITY OF TECHNOLOGY



FAKULTA CHEMICKÁ
ÚSTAV CHEMIE MATERIÁLŮ

FACULTY OF CHEMISTRY
INSTITUTE OF MATERIALS SCIENCE

RHEOLOGICAL PROPERTIES OF BIODEGRADABLE THERMOSENSITIVE COPOLYMERS

REOLOGICKÉ VLASTNOSTI BIODEGRADABILNÍCH TERMOCITLIVÝCH KOPOLYMERŮ

DIPLOMOVÁ PRÁCE

MASTER'S THESIS

AUTOR PRÁCE

AUTHOR

Bc. IVANA CHAMRADOVÁ

VEDOUCÍ PRÁCE

SUPERVISOR

Ing. LUCY VOJTOVÁ, Ph.D.

BRNO 2012



Vysoké učení technické v Brně
Fakulta chemická
Purkyňova 464/118, 61200 Brno 12

Zadání diplomové práce

Číslo diplomové práce:	FCH-DIP0636/2011	Akademický rok: 2011/2012
Ústav:	Ústav chemie materiálů	
Student(ka):	Bc. Ivana Chamradová	
Studijní program:	Chemie, technologie a vlastnosti materiálů (N2820)	
Studijní obor:	Chemie, technologie a vlastnosti materiálů (2808T016)	
Vedoucí práce	Ing. Lucy Vojtová, Ph.D.	
Konzultanti:		

Název diplomové práce:

Reologické vlastnosti biodegradabilních termocitlivých kopolymerů

Zadání diplomové práce:

Literární rešerše na téma reologie gelujících polymerů

Sledování změn reologických vlastností termocitlivých kopolymerů modifikovaných jak anhydridem kyseliny itakonové tak i přidavkem anorganického plniva

Vyhodnocení naměřených dat

Závěry

Termín odevzdání diplomové práce: 11.5.2012

Diplomová práce se odevzdává ve třech exemplářích na sekretariát ústavu a v elektronické formě vedoucímu diplomové práce. Toto zadání je přílohou diplomové práce.

Bc. Ivana Chamradová
Student(ka)

Ing. Lucy Vojtová, Ph.D.
Vedoucí práce

prof. RNDr. Josef Jančář, CSc.
Ředitel ústavu

V Brně, dne 15.1.2012

prof. Ing. Jaromír Havlica, DrSc.
Děkan fakulty

ABSTRACT

The general goal of the proposed diploma work was preparation, characterization and rheological study of well-defined “smart” injectable hydrogels from biodegradable, biocompatible, controlled life-time copolymers based on hydrophilic poly(ethylene glycol) (PEG) and hydrophobic poly(lactic acid)—*co*—poly(glycolic acid) (PLA/PGA) copolymer. Resulted thermosensitive PLGA—PEG—PLGA copolymer, which gels at body temperature, was additionally functionalized by itaconic anhydride (ITA) from renewable resources, bringing both reactive carbon double bonds and functional —COOH groups to polymer ends. Additionally, the PLGA—PEG—PLGA copolymer was modified by inorganic bioactive hydroxyapatite (HAp) for usage as injectable bone bioadhesive. Both functionalized ITA/PLGA—PEG—PLGA/ITA copolymer and PLGA—PEG—PLGA/HAp polymer composite affected rheological properties of original PLGA—PEG—PLGA copolymer deciding whether or not would be the new polymeric material suitable as injectable drug carrier or bone adhesive in medical applications.

Experimental part of this thesis describes mainly characterization of viscoelastic properties of both unmodified and ITA or HAp modified PLGA—PEG—PLGA copolymer by test tube inverting method (TTIM) and dynamic rheological analysis. Advantage of TTIM is sol-gel visualization with determination of the critical gelation temperature and the critical gelation concentration. The rheological measurements provide information about viscosity and elasticity of the gel by the changes storage (G') and loss (G'') modulus. The prepared copolymers were additionally characterized by ^1H NMR and GPC. Surface and HAp particles size was determined by both SEM and Laser Particles Size Analyzer.

Both unmodified and ITA or HAp modified PLGA—PEG—PLGA copolymers exhibited sol-gel transitions induced by increasing temperature. Rheological properties of copolymers' 6 to 24 wt % water solutions investigated either by TTIM or by rheometer were in good agreement. Evaluating by rheometer, the copolymers showed two cross-points, where $G' = G''$. The first one very well corresponded with the first sol-gel transition found via TTIM. The maximum values of G' representing the highest gel stiffness lie in the white gel observed by TTIM. The second cross-point constituted to the gel-suspension transition where white polymer is precipitated from the water. The gel stiffness grows with increasing polymer concentration in water. In comparison, ITA modification or addition of HAp (0, 10, 20, 30, 40, 50 wt %) caused increasing the gel stiffness of unmodified PLGA—PEG—PLGA copolymer and approximating the temperature of G'_{max} closer to body temperature (37 °C).

Investigated both ITA/PLGA—PEG—PLGA/ITA copolymer and PLGA—PEG—PLGA/HAp composite were proved to be suitable candidates as injectable systems for drug delivery or regenerative medicine in orthopedics or dental applications, respectively.

KEY WORDS

biodegradable polymers, sol-gel transition, hydroxyapatite, rheology, bone adhesive

ABSTRAKT

Hlavním cílem předložené diplomové práce byla příprava, charakterizace a reologická studie "inteligentních" injektovatelných hydrogelů, které jsou biodegradovatelné, biokompatibilní a s řízenou životností sestávajících se z hydrofilního polyethylenglykolu (PEG) a hydrofobního kopolymeru kyseliny polymléčné a polyglykolové (PLA/PGA). Výsledný termosenzitivní PLGA—PEG—PLGA kopolymer, který geluje při teplotě lidského těla, byl dále funkcionalizován anhydridem kyseliny itakonové získané z obnovitelných zdrojů, přinášející jak reaktivní dvojně vazby tak i funkční —COOH skupiny na konce kopolymeru. Navíc byl PLGA—PEG—PLGA kopolymer modifikován bioaktivním anorganickým hydroxyapatitem pro použití jako injektovatelné kostní adhezivum. Oba modifikované kopolymery jak ITA/PLGA—PEG—PLGA/ITA tak i PLGA—PEG—PLGA/HAp ovlivňují reologické vlastnosti původního PLGA—PEG—PLGA kopolymeru rozhodující o tom, zda by mohly být nové polymerní materiály vhodné jako injektovatelné nosiče léčiv nebo kostní lepidla v lékařských aplikacích. Experimentální část této práce je zaměřena především na charakterizaci viskoelastických vlastností jak nemodifikovaného PLGA—PEG—PLGA kopolymeru tak i s přidáním ITA nebo HAp metodou obrácených testovacích vialek (TTIM) a dynamickou reologickou analýzou. Výhodou TTIM je vizualizace přechodu sol-gel, určení kritické gelační teploty a kritické gelační koncentrace. Reologická měření poskytují informace o viskozitě a vizkoelasticitě gelu změnou elastického (G') a ztrátového (G'') modulu. Připravené kopolymery byly také charakterizovány ^1H NMR a GPC. Povrch a velikost částic HAp byl popsán pomocí SEM a laserového analyzátoru částic.

Původní PLGA—PEG—PLGA kopolymer i kopolymer modifikovaný ITA a HAp vykazovaly sol-gel přechod vyvolaný zvýšením teploty. Reologické vlastnosti kopolymerů v koncentračním rozmezí 6 až 24 hm. % ve vodě byly studovány buď TTIM nebo užitím reometru a získané výsledky spolu velmi dobře korespondovaly. Reologické vyhodnocení prokázalo dvě „překřížení“, kde $G' = G''$. První překřížení velmi dobře korespondovalo s prvním sol-gel přechodem nalezeným prostřednictvím TTIM. Maximální hodnota G' odpovídající nejvyšší tuhosti polymerního gelu byla situována v bílém gelu. Druhý fázový přechod představuje přechod mezi gelem a suspenzí, kdy je bílý polymer oddělen od vody. Tuhost gelu roste s rostoucí koncentrací polymeru ve vodě. Pro srovnání, kopolymer modifikovaný jak ITA, tak i přidáním HAp (0, 10, 20, 30, 40, 50 hm %) vykázal zvýšení tuhosti gelu oproti původnímu kopolymeru PLGA—PEG—PLGA a přiblížení teploty maximální hodnoty G' tělesné teplotě (37 °C).

Bylo prokázáno, že jak ITA/PLGA—PEG—PLGA/ITA kopolymer tak i PLGA—PEG—PLGA/HAp kompozit jsou vhodnými kandidáty na injektovatelné systémy pro řízené uvolňování léčiv či kostní adhezivum pro ortopedii nebo zubní aplikace.

KEY WORDS

biodegradabilní polymery, sol-gel přechod, hydroxyapatit, reologie, kostní adhezivum

CHAMRADOVÁ, I. *Rheological properties of biodegradable thermosensitive copolymers*. Brno: Brno University of Technology, Faculty of Chemistry, 2012. 62 s. Supervisor Ing. Lucy Vojtová, Ph.D.

DECLARATION

I declare that the diploma thesis has been worked out by myself and that all the quotations from the used literary sources are accurate and complete. The content of the diploma thesis is the property of the Faculty of Chemistry of Brno University of Technology and all commercial uses are allowed only if approved by both the supervisor and the dean of the Faculty of Chemistry, BUT.

.....
student's signature

Acknowledgement

I would like to thank my supervisor Ing. Lucy Vojtová, Ph.D. for professional advice, exceptional patience and the whole time which she has given to me. I also thank Ing. Petr Poláček, Ph.D for his willingness and help in understanding rheological measurements. I would like to thank my colleagues from the laboratory for their friendship and help. I express my thanks to my dear mother and my boyfriend for their support during the study.

CONTENT

1	INTRODUCTION	7
2	THEORETICAL PART	9
2.1	Biodegradable Polymers	9
2.1.1	Natural Polymers	9
2.1.2	Synthetic Polymers	10
2.1.3	Temperature-responsive Hydrogel	11
2.1.3.1	Diblock Copolymers (AB)	12
2.1.3.2	Triblock Copolymers (ABA/BAB)	12
2.1.4	Micelle Formation	13
2.1.5	Determination of Critical Micelle Concentration	14
2.1.6	PLGA—PEG—PLGA Functionalization	14
2.1.6.1	Itaconic Anhydride	14
2.2	Resorbable Composites for Bone Tissue Engineering	15
2.2.1	Bone Structure	16
2.2.2	Inorganic Component	17
2.2.2.1	Bioactive Glass	18
2.2.2.2	Ceramics	18
2.2.2.3	Bioactive Glass-Ceramics	18
2.2.2.4	Metal	18
2.2.2.5	Hydroxyapatite	19
2.2.3	Biodegradable Polymer/hydroxyapatite Composite	20
2.2.3.1	HAp/polymer Solution	20
2.2.3.2	Silanization of HAp-surface	20
2.2.3.3	Synthesis of Core-shell Nanospheres	20
2.3	Polymer Rheology	21
2.3.1	Polymeric Liquids	21
2.3.2	Newtonian Fluids	21
2.3.3	Non-Newtonian Fluids	21
2.3.4	Viscoelastic Behavior of Polymeric Solution	22
2.3.4.1	Linear Viscoelastic Region	23
2.3.4.2	Oscillatory Tests with a Maxwell Model	24
2.3.5	Gelation Behavior of PLGA—PEG—PLGA	26
2.4	Goal of the Work	26
3	EXPERIMENTAL PART	27
3.1	Chemicals	27
3.2	Equipments	27
3.3	Methods	28
3.3.1	Synthesis of PLGA—PEG—PLGA Copolymer	28
3.3.2	Preparation of ITA/PLGA—PEG—PLGA/ITA Copolymer	28

3.3.3	Samples Purification	28
3.3.4	Preparation of Copolymer Water Solution.....	28
3.3.5	Preparation of PLGA—PEG—PLGA/HAp Composites.....	28
3.4	Characterization.....	28
3.4.1	Scanning Electron Microscope (SEM).....	28
3.4.2	Laser Particle Size Analyser	29
3.4.3	Proton Nuclear Magnetic Resonance (¹ H NMR).....	29
3.4.4	Gel Permeation Chromatography (GPC)	29
3.4.5	Test Tube Inverting Method (TTIM)	29
3.4.6	Dynamic Rheological Analysis.....	30
4	RESULTS AND DISSCUSSION	31
4.1	Characterization of Copolymers.....	31
4.1	Characterization of HAp Particles	32
4.2	Gel Point Determination.....	34
4.2.1	Test Tube Inverting Method.....	34
4.2.1.1	PLGA—PEG—PLGA Copolymers.....	34
4.2.1.2	ITA/PLGA—PEG—PLGA/ITA Copolymer.....	36
4.2.1.3	PLGA—PEG—PLGA/HAp Composite	36
4.2.2	Dynamic Rheological Analysis.....	37
4.2.2.1	Linear Region.....	37
4.2.2.2	Stress Sweep.....	37
4.2.2.3	Frequency Sweep	38
4.2.3	PLGA—PEG—PLGA Copolymers.....	40
4.2.3.1	Influence of Purifying Agents	40
4.2.4	ITA/PLGA—PEG—PLGA/ITA Copolymer.....	43
4.2.5	PLGA—PEG—PLGA/HAp Composites.....	46
5	CONCLUSION.....	49
6	REFERENCES	50
7	APPENDICES	58
7.1	The List of Pictures	58
7.2	The List of Tables.....	60
7.3	The List of Abbreviations	61
7.4	The List of Symbols.....	62

1 INTRODUCTION

Biodegradable synthetic polymers offer a number of advantages over materials for developing scaffolds in tissue engineering. The key advantages include the ability to tailor mechanical properties and degradation kinetics to suit various applications. Synthetic polymeric biomaterials are easy to produce in various shapes, reasonable cost and in wide range of physical and mechanical properties. Hence biodegradable polymers are attractive candidate materials for short-term medical applications like sutures, drug delivery devices, orthopedic fixation devices, wound dressings, temporary vascular grafts, stents etc. [1].

Thermosensitive copolymers based on the poly(ethylene glycol) and poly(lactic-*co*-glycolic acid) (PLGA-PEG-PLGA) have been extensively studied. Copolymers are biocompatible and biodegradable in the human body and thus applicable for the controlled drug delivery system or injectable materials for regenerative medicine. These bioresorbable polymers that are fully degradable into the body's natural metabolites by simple hydrolysis under physiological conditions are the most attractive scaffold materials. PLGA-PEG-PLGA copolymers have been extensively investigated as biomaterials for bone tissue regeneration and reconstruction [2].

In recent years, the search for innovative bone substitutes for developing this new therapeutic concept has concentrated on non-metallic composite materials such as polymer/ceramic composites. These materials link the advantages of polymers (structural stability, strength, biocompatibility, desired shape) with properties of ceramics that resemble those of bone structure. One of the most important groups of polymer/ceramic composites are polymer/HAp materials. HAp has excellent biocompatibility and bioactivity and has been widely used in medical, dental, and other health-related fields as material for damaged bones or teeth, important implant and scaffold materials and drug delivery agents due their biological similarity to natural tissues. [3].

The aim of presented work is study of the rheological properties of poly(D,L-lactic acid-*co*-glycolic acid)-*b*-poly(ethylene glycol)-*b*-poly(D,L-lactic acid-*co*-glycolic acid) (PLGA-PEG-PLGA), which was either functionalized with itaconic anhydride or modified by hydroxyapatite. The gel point of newly synthesized thermosensitive copolymers were evaluated by both test tube inverting method (TTIM) and rheometer. Comparisons these two methods help us to better understand the sol-gel transitions in polymer systems and to determine whether or not these materials are appropriate as an injectable biomedical hydrogels.

2 THEORETICAL PART

2.1 Biodegradable Polymers

Polymeric biomaterials firstly introduced into clinical use in 1960s as sutures, plates and fixtures for fraction fixation devices [4, 5, 6, 7]. The advantages of polymeric biomaterials, compared to metallic or ceramics materials, are simple manufacturing of orthopedics products in various shapes, adequate cost and wide range of physical and mechanical properties [8, 99].

Biodegradable polymers are materials with the ability to function for a temporary period and subsequently degrade, under a controlled mechanism, into products easily eliminated in the body's metabolic pathways. In this way, biodegradability not only eliminates the risk of complications associated with the long-term presence of a foreign material and the need for a second surgery for implant removal. In the last decade are utilized most frequently for tissue engineering, controlled drug delivery system or injectable materials in regenerative medicine [4]. Polymers may be obtained from natural sources or synthetic processes.

2.1.1 Natural Polymers

The natural-based materials are biopolymers which include proteins such as collagen, gelatin, fibrin and polysaccharides (alginate, hyaluronic acid, agarose, chitosan) (Fig. 1).

Collagen occurs as major component of connective tissue (such as bones, cartilage, blood vessels), giving strength and flexibility. However, collagen has been actively investigated as the favorable artificial microenvironment for bone ingrowth [10, 11, 12].

Gelatin is denatured protein obtained by acid and alkaline processing of collagen. There are two types of gelatin types - acid pretreatment (Type A gelatin) uses pigskin whereas alkaline treatment (Type B gelatin) makes use of cattle hides and bones [13].

Fibrin (protein matrix produced from fibrinogen) is utilized in research in tissue engineering due to their innate ability to induce improved cellular interaction e.g. substrate for cell adhesion, spreading, migration and proliferation [14, 15].

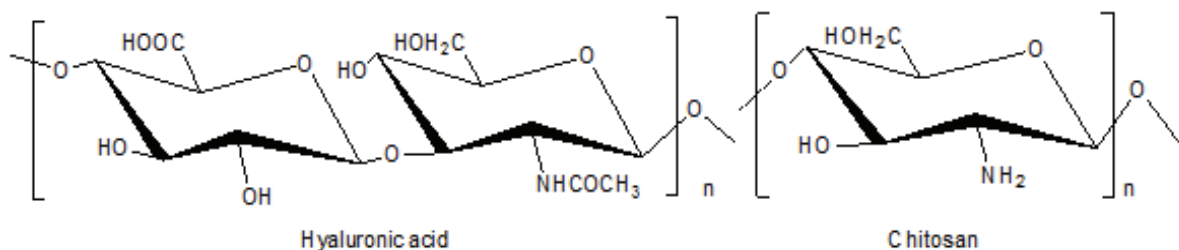


Fig. 1 Natural polymers.

Polysaccharides are class of biopolymers constituted by simple sugar monomers. Differences in the monosaccharide composition, chain shapes and molecular weight dictate their physical properties e.g. solubility, gelation, surface properties and degradation time [16, 17].

2.1.2 Synthetic Polymers

Synthetic materials indeed provide excellent chemical and mechanical properties than natural polymers. One of the greatest advantages is the ability to manage process of synthesis such as molecular weights, functional groups, configuration and conformations of polymer chains. Tailoring polymer structure can determinate the length and degradation characteristics. Degradation of synthetic polymers may be caused via hydrolytic pathway or enzymatic cleavage [18].

Polymers of α -hydroxy esters as PLA (from D,L-LA or L-LA), PGA or their copolymers (PLGA) are the most widely investigated synthetic biodegradable polymers for tissue engineering. The other polymers are poly(ϵ -caprolactone) [19], poly(propylene fumarate) (PPF) [20, 21], poly(phosphazene) [22], poly(hydroxyethyl methacrylate) (PHEMA) [23]. The typically synthetic biodegradable polymers are summarized in Table 1.

Table 1: Physical properties of biodegradable polymers [24, 25]

	Melting point °C	T_g (°C)	Degradation time (month)	Polymer repeats unit structure
L – PLA (Semicryst.)	173 - 178	60 - 65	> 2 years	$\left[\text{O}-\underset{\text{CH}_3}{\text{CH}}-\overset{\text{O}}{\parallel}{\text{C}} \right]_n$
D, L – PLA (Amorphous)	-	55 - 60	12 - 16	
PGA	225 - 230	35 - 40	3 - 4	$\left[\text{O}-\text{CH}_2-\overset{\text{O}}{\parallel}{\text{C}} \right]_n$
PLGA*	173 - 200 **	50 - 55	< 3 3 - 6 ^b	$\left[\text{O}-\text{CH}_2-\overset{\text{O}}{\parallel}{\text{C}}-\text{O}-\underset{\text{CH}_3}{\text{CH}}-\overset{\text{O}}{\parallel}{\text{C}} \right]_n$
PEG	43 ^a	-	-	$\left[\text{CH}_2-\text{CH}_2-\text{O} \right]_n$
PCL	50 - 63	-60	< 24	$\left[\text{O}-\left(\text{CH}_2 \right)_5-\overset{\text{O}}{\parallel}{\text{C}} \right]_n$
PPF	30 - 50	-60	> 24	$\left[\text{O}-\overset{\text{O}}{\parallel}{\text{C}}-\text{HC}=\text{CH}-\overset{\text{O}}{\parallel}{\text{C}}-\text{O}-\underset{\text{CH}_3}{\text{CH}} \right]_n$

T_g – glass transition temperature

^a for PEG with molecular weight $M_n = 1500 \text{ g mol}^{-1}$

^b degradation time change according to the ratio of LA and GA

* PLGA consists of PGA and L-LA form [26]

** PLGA melting point depends on the composition molar ratio of PLA and PGA

Synthetic polymers are also very attractive due to the fabrication into the various shapes (sutures, scaffold, porous materials and fibrous scaffold) and designing with a chemical functional group [2, 25]. Copolymers based on the hydrophobic PLA, PGA and hydrophilic poly(ethylene glycol) (PEG) have been published as the thermoreversible biodegradable gels by Lee et al. [27]. The aqueous solution of this copolymer is a free flowing sol at room temperature but it becomes a gel at body temperature (37 °C) resulting in reversible sol-gel transition characterized by the gelation phase diagram.

2.1.3 Temperature-responsive Hydrogel

Temperature-responsive (or thermogelling) copolymers exhibit a phase change behavior of sol-gel-sol, sol-gel or gel-sol transition with increasing/decreasing temperature. The phase transition can be adjusted by different parameters such as molecular weight of homopolymer/copolymer, composition of copolymer, concentration of polymer solution, solvent etc. The sol-gel transition is very attractive transition for medical applications because the bioactive agents (e.g. inorganic components, drug, healing medicament) can be mixed in the aqueous copolymer solutions (sol phase) at low temperature and injected into the body where higher body-temperature would lead to the formation of a gel. Degradation (diffusion or erosion) of copolymer gel can control release of agents [28, 29, 30].

Thermogelling copolymers behave in different molecular architectures such as AB diblock, ABA/BAB triblock, graft copolymer, star-shape block, multi-block and branched copolymer (Fig. 2) [31]. As biodegradable thermogelling polymers the poly(D, L—lactid acid-co-glycolid acid)/poly(ethylene glycol) (PLGA—PEG—PLGA) [27], poly(ethylene glycol)/polycaprolactone (PEG—PCL) [32] and, poly(ethylene glycol)/poly(propylene fumarate) (PEG—PPF) [33] are mostly studied.

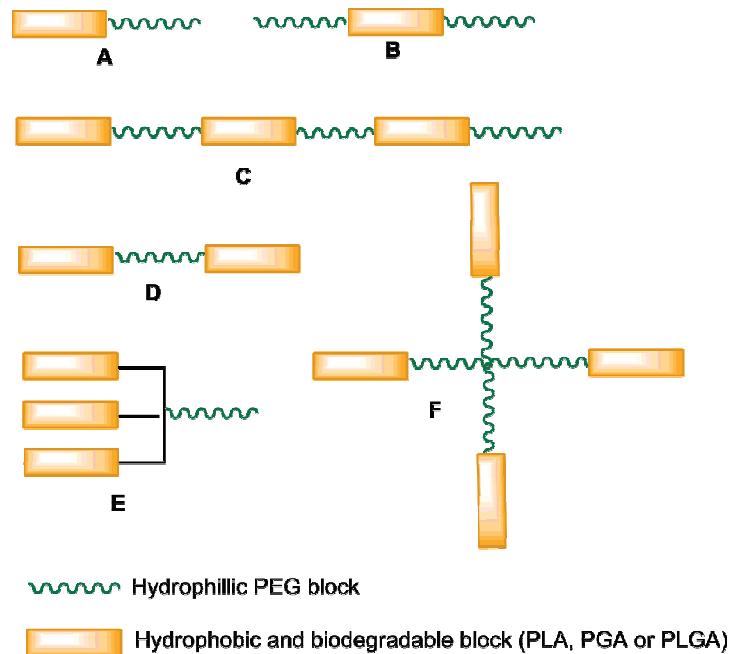


Fig. 2 Schematic presentation of block copolymer structure (a) A-B diblock, (b) A-B-A triblock, (c) B-A-B triblock, (d) alternating multiblock, (e) multi-armed structure, (f) star-shape block.

2.1.3.1 Diblock Copolymers (AB)

Block copolymers consisting of a hydrophilic A segment (PEG) and hydrophobic polyester segment B (PLLA, PLGA, PCL, PPO). Hydrophobic blocks are separated from the aqueous surrounding to form an inner core and hydrophilic segments consist of a wall around it [34].

Choi et al. synthesized via ring opening polymerization PEG—PLLA, PEG—P(LLA/GA) and PEG—P(DLLA/GA) diblock copolymers and the sol-gel transition properties of these diblock copolymer were influenced by the hydrophilic/hydrophobic balance. Aqueous solutions of PEG_x—PLLA_x diblock copolymers exhibited gel-to-sol transition with increasing temperature [35].

2.1.3.2 Triblock Copolymers (ABA/BAB)

The ABA-type triblock copolymers with central PEG demonstrated an interesting reversible sol to gel and gel to sol transition in aqueous solution, where A stands for hydrophobic blocks and B for hydrophilic blocks (Fig. 3).

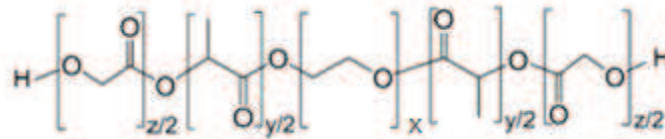


Fig. 3 Formula of ABA-type triblock copolymer PLGA—PEG—PLGA.

Lee and Shim [36, 39] studied the solubility of triblock copolymers with central PEG ($M_n = 1000 \text{ g}\cdot\text{mol}^{-1}$) block with different molecular weight of PLGA block. The PLGA with ($M_n = 1600 \text{ g}\cdot\text{mol}^{-1}$) was insoluble in water, while triblock copolymer with PLGA block ($M_n = 900 \text{ g}\cdot\text{mol}^{-1}$) and lower was soluble in water but do not form hydrogel in water. The solubility of polymer depends strongly on the molecular weight of PLGA block.

The subject of study were also triblock copolymers with different PEO/PLGA ratios and a constant D,L—LA/GA ratio. The longer PLGA chain in the triblock copolymers causes the stronger hydrophobic interaction, leading to an increase in the association tendency. In other words the CGC increases with an increasing PEO/PLGA ratio. *Critical gelation concentration* (CGC) defined as the minimum copolymer concentration in aqueous solution at which the gel is observed. They investigated changes in phase transition temperature at varying D,L—LA/GA ratios with same PEG/PLGA ratio (PLGA/PEG = 2.7). The CGC increases and critical gelation (CGT) goes to lower temperature with decreasing D,L—LA/GA ratios. The CGT is lowest temperature above which the formation of the gel. With increasing content of GA block increases hydrophilicity whole PLGA block. The CGC for ABA-type is determined by PEG/PLGA ratio [36] (Fig. 4).

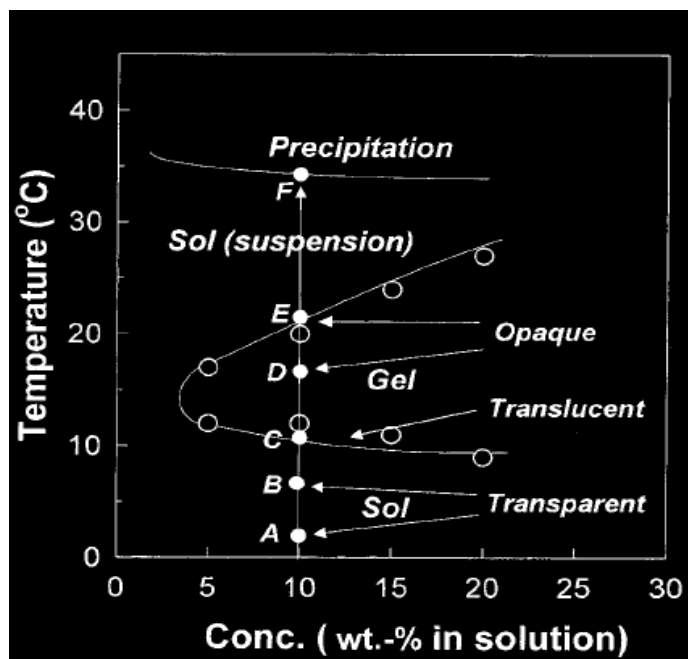


Fig. 4 A typical phase diagram of ABA-type PLGA-block-PEO-block-PLGA triblock copolymer in water [36].

In 2010 Yu and coworkers studied rheological behavior of PLGA—PEG—PLGA copolymers, which were separated in a good solvent (chloroform or methylene chloride) and precipitated in poor solvent (methanol, hexane, diethyl ether). Products separated via different precipitate agents might exhibit significantly different physical behaviors. The obtained products exhibited significantly different macroscopic states in water: some were sols, some were precipitates and some underwent sol–gel transition upon heating. It were observed that the different precipitated agent used in polymer separation have a significant influence on the gel stiffness detected by shear storage modulus (G') [37].

The same authors studied the effect of polymer degradation on the gelation properties of PLGA—PEG—PLGA by dynamic rheological measurements or by the test tube inverting method. Aqueous copolymer solution of 20 wt % synthesized at 130 and 160 °C spontaneously formed opaque gel and transparent gel at body temperature. After degradation process storage modulus decrease with time and maximum of G' was shifted to the higher temperature [38].

2.1.4 Micelle Formation

Micellar gelation mechanism of formation was studied by dynamic light scattering (DLS). Shim and coworkers studied the micellar formation of the most used PLGA—PEG—PLGA triblock copolymer with commercial name Regel® [39].

The mechanism is illustrated in Fig. 5. At low temperature (in sol state) lower than GCT unimers and individual micelles were observed (A). With the increasing temperature the grow size of micelles (B) and the micelles' aggregates formed a close packed structure led to a sol-gel transition (C). The aggregation and packing interactions between micelles increase along with changing the color from translucent to white gel (C and D). Further raising in temperature leads to corona-decomposition (E) caused by dehydration of PEG-block. The over shrunk micelle groups in water were observed (F) [36, 39].

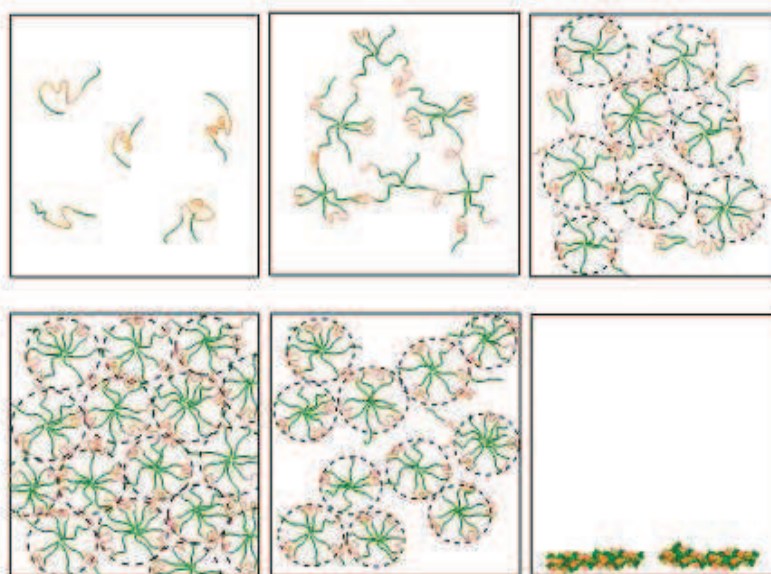


Fig. 5 Micellar gelation mechanisms for ABA-type triblock copolymer in aqueous solution.

2.1.5 Determination of Critical Micelle Concentration

Critical micelle concentration (CMC) is defined as the concentration of copolymers above which micelles are spontaneously formed. The micellization was studied by the hydrophobic dye, 1,6-diphenyl-1,3,5-hexa-triene (DPH) in low-concentrated polymer solution. The critical micellization concentration (CMC) value for PLGA—PEG—PLGA copolymers by absorbance at 378 nm relative to 400 nm was determined [37, 40].

2.1.6 PLGA—PEG—PLGA Functionalization

While PLGA—PEG—PLGA thermoreversible gels increase the hydrogel applicability as injectable implants and biodegradable matrix for the controlled drug delivery systems without surgery, on the other hand, the reversible physical network, the phase-transition temperature range and low degree of functionality limit the application for other branches. Therefore, functionalization (even by inorganic material) and chemical cross-linking of these polymers is being of great interest because it might expand the possible applications. In order to obtain crosslinkable functionalization, hydroxyl-terminated poly(ϵ -caprolactone), PLA and PGA have been modified with maleic anhydride [41] and [42], fumaric acid [41], acrylates [43], methacrylic anhydride [44] and (3-isocyanatopropyl)triethoxysilane [45] and [46]. The use of itaconic anhydride (ITA) has been published only in case of modifying poly(ϵ -caprolactone) [42] or recently by our group, where functionalization conditions of PLGA—PEG—PLGA by ITA were studied [47].

2.1.6.1 Itaconic Anhydride

Itaconic anhydride (ITA) can be gained from renewable resources by pyrolysis of citric acid or by fermentation of polysaccharides by *Aspergillus terreus*. [48]. It is known that ITA undergoes degradation at physical condition to non-toxic products. At the beginning the itaconic anhydride hydrolyses in water to itaconic acid. Adler et al. studied the complete

oxidation of itaconic acid by Mitochondria from guinea pig liver in the presence of Mg^{2+} . They observed acetate, lactate and carbon dioxide as main degradation products [49].

ITA brings carboxyl groups for bioactive compounds bonding and double bonds suitable for chemical cross-linking to the ends of copolymer. We have reported [47] the positive effect of the presence of $-COOH$ groups at the end of ITA/PLGA—PEG—PLGA/ITA on the physical cross-linking and thus on sol-gel phase transition in comparison with unmodified PLGA—PEG—PLGA. Prepared ITA/PLGA—PEG—PLGA/ITA macromonomers (see Fig. 6) are light, temperature and pH sensitive and can be cross-linked either chemically by covalent bonding through the double bonds (e.g. via photopolymerization) and/or physically (by hydrogen bond or ionic interactions) in order to produce new functionalized 3D-hydrogel network. Moreover, functional $-COOH$ groups can be used as coupling sites for increasing hydrogel's biocompatibility, bioinductivity, adhesion or other physical properties and thus might be "tailored" for a certain type of biomedical applications such as injectable polymer drug delivery systems, tissue implants or resorbable bone adhesives.

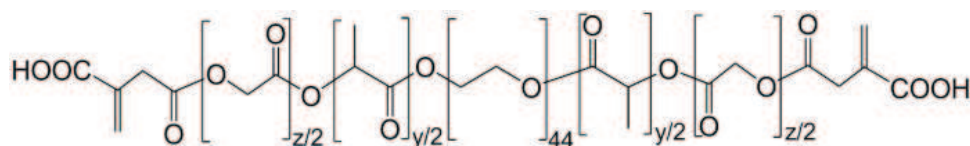


Fig. 6 Chemical structure of ITA/PLGA—PEG—PLGA/ITA, where $M_n(PEG) = 1\ 500\ g\cdot mol^{-1}$

Moreover, the PLGA—PEG—PLGA copolymer might be modified by bioactive inorganic particles in order to prepare polymer/ceramic composite as a bone cell supporting matrix. This biocompatible heterogeneous polymer composite with suitable mechanical properties are useful for bone regeneration in tissue engineering.

2.2 Resorbable Composites for Bone Tissue Engineering

The main goal of bone tissue engineering has been to develop biodegradable materials as bone graft substitutes for filling large or small bone defect [23, 50, 51] which can be caused by disease, tumor, infections or fractures [52, 53]. The biocomposites could be classified based on their biodegradability as fully or partially resorbable and nonresorbable.

Resorbable biocomposites could be used for internal fracture fixation applications with degradation inside the body in a controllable rate. *Partially resorbable* composites could be composed of a non-absorbable reinforcing materials and fully resorbable matrix materials (e.g. PLA with HAp, PHB and alumina or calcium carbonate). *Non-resorbable* biocomposites provide specific mechanical properties and stability (knee joint prostheses, dental posts, stems of hip) (Fig. 7).

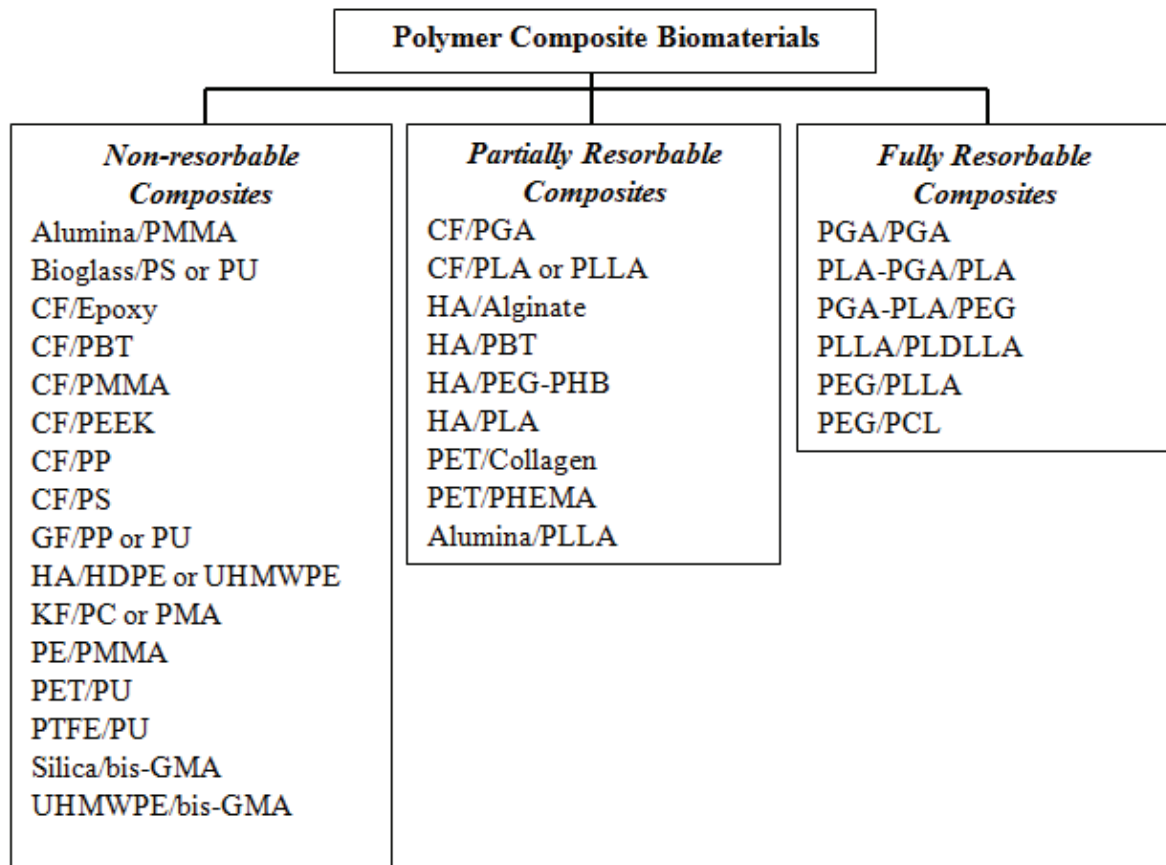


Fig. 7 Clasiffication of non-resorbable, partially and fully resorbable composites [10].

2.2.1 Bone Structure

The bone is an anisotropic, heterogeneous, viscoelastic material and their composition depends on a large number of factors: the age, sex, type of bone tissue (trabecular, cortical etc.) or the species. Mechanical properties of tissue are summarized in Table 2.

Table 2: Mechanical properties of hard and soft tissue [10, 54].

	Type of tissue	Elastic modulus (GPa)	Tensile strength (MPa)
Hard tissue	cortical bone	12.8 – 17.7	52 – 133
	enamel	84.3	10
	dentine	11	39.3
Soft tissue	cartilage	10.5	27.5
	ligament	303	29.5
	tendon	401.5	46.5
	collagen (dry)	1.8 – 2.25	-
Substitutes	PGA	-	57
	L-PLA	-	59 – 72
	D,L-PLA	-	44

Human or animal bones are an *inorganic/organic* material consisting from collagen, calcium phosphate and water [54, 55]. Organic components of bone include cells (osteocytes) collagen fibers, which contribute to the flexibility and tensile strength of bone. Inorganic components make up 65% of bone by mass, and consist of hydroxyapatite, a mineral salt that is largely calcium phosphate, which accounts for the hardness and compression resistance of bone (Fig. 8).

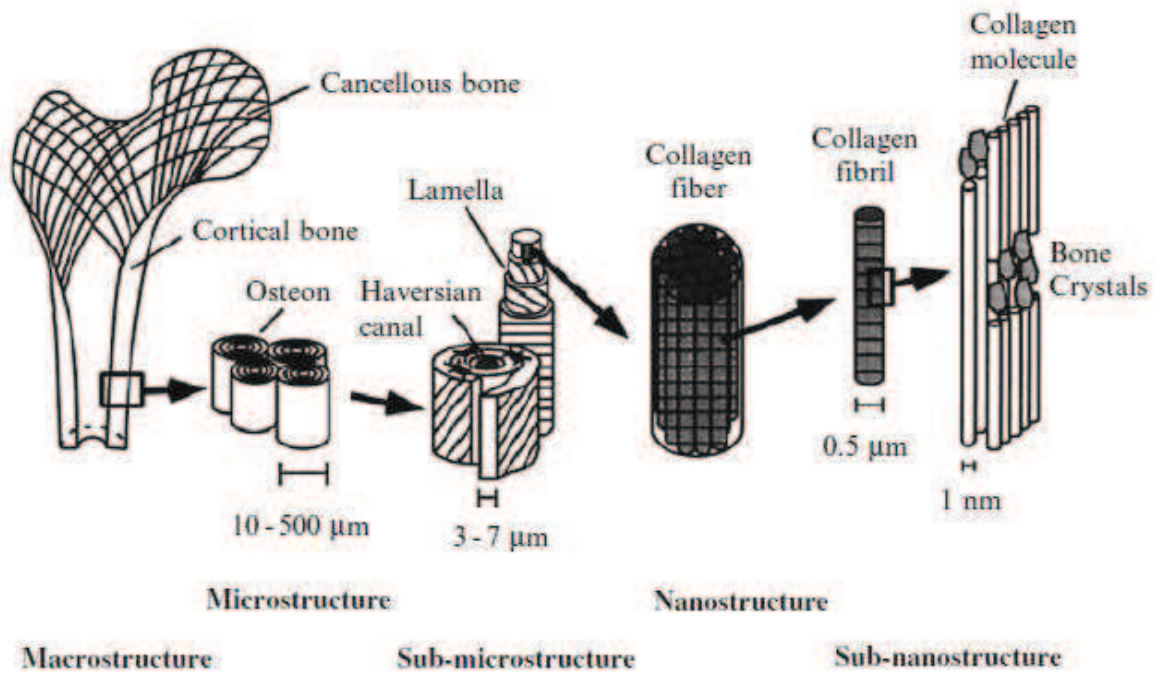


Fig. 8 Skeletal system structure of a human bone [6].

Bones support the body and cradle the soft organs, protect vital organs, store minerals such as calcium and phosphate, and house hematopoietic tissue in specific marrow cavities [6].

2.2.2 Inorganic Component

The regeneration of load-bearing bones, the use of biodegradable polymer scaffolds is challenging because of their low mechanical strength. This gave rise to inorganic/organic scaffold. The commonly reinforcement of biodegradable polymers is hydroxyapatite [56], bioceramics [57], bioglass [58], glass-ceramics [59] and metals [60].

Metallic materials and ceramics have been used, as bone implants for long time but disadvantages are high elastic modulus, loosening of the prosthesis, lack of biodegradability in biological environment which have led to the development of materials that would be far more tolerant of human bone [50, 61].

2.2.2.1 Bioactive Glass

Bioactive glass has an amorphous structure, whereas are crystallized glasses, consisting of a composite of a crystalline phase and a residual glassy phase. The bioactive glass-scaffolds with interconnected porosity undergoes specific surface reactions when implanted into the body leading to the formation of an HA-like layer that is responsible for the formation of a firm bond with hard and soft tissues [62]. The most commonly bioglass is designed from silicate, borate or phosphate glasses. The commercial name Bioglass® has been the most widely researched glass for biomedical applications [63]

2.2.2.2 Ceramics

The first generation is formed by *inert ceramics* consisting from alumina and zirconia. They are primarily used to replace damaged of femoral heads [4]. Although the ceramics' implants are biocompatible, the body will react against them for their foreign nature and these ceramics are surrounded by collagen capsule which is isolated from the body. These ceramics' implants have never HAppened equivalent substitute for bone [64].

Research in bioceramics brought promising results in 1980. One of common characteristics of bioceramics is their surface reactivity. During implantation, reactions occur at the material/tissue interfaces that lead to time-dependent changes in the surface characteristics of the implanted materials. It contributes to their bone bonding ability and their enhancing effect on bone tissue formation [65]. There are many forms of ceramics for medical applications e.g. powders, porous pieces and injectable mixtures [66].

2.2.2.3 Bioactive Glass-Ceramics

On the other hand, glass ceramics containing crystalline apatite ($\text{Ca}_{10}(\text{PO}_4)_6\text{O,F}_2$) and wollastonite ($\text{CaO}\cdot\text{SiO}_2$) in $\text{MgO}\text{-CaO}\text{-SiO}_2$ glassy matrix has unique mechanical strength. These materials usually possess a very fine microstructure, containing few or no residual pores, these features resulting in improved mechanical properties in the end-product [3, 67]. They are used in orthopedics, neurosurgery or in dentistry. Bioactivity of glass-ceramics is attributed to apatite formation on its surface. Dissolution of calcium and silicate ions from the glass ceramics plays very important role in the forming the surface apatite-layer [67, 68]. The commercial products of glass-ceramics are Japanese Cerabone® or Czech BAS-O [69,70].

2.2.2.4 Metal

Metal alloys used in surgical implants must exhibit unique properties such a good mechanical strength, high corrosion and wear resistance, biocompatibility and safety. The most frequently used alloys like stainless steel [71, 68], cobalt-chromium [72] and titanium alloys [73] and Ni-alloys [74, 75] are utilized in biomedical and dental applications (Fig. 9). The elastic moduli of current metallic biomaterials are not well matched with that of natural bone tissue resulting in reduced stimulation of new bone and remodeling [76, 77].



Fig. 9 (a) Metal prosthesis [77], (b) ceramic orthopaedic implants [78], (c) 3-dimensional biomass-scaffold [79], (d) glass-ceramic crown used in dental applications [80].

2.2.2.5 Hydroxyapatite

Hydroxyapatite (HAp) $\text{Ca}_{10}(\text{PO}_4)_6(\text{OH})_2$ is one of the most bioceramics that is chemically similar to human inorganic hard tissue and used in medical and dental applications. The natural sources of HAp are animal bones and corals or can be synthesized from appropriate substrates. HAp materials made from animal bones inherit some properties such as chemical composition and structure [81, 82]. Synthetically produced HAp is preferable for their controlled microstructure, uniform composition and high biocompatibility [83]. It has been used clinically in a nanostructure form - powders (Fig. 10), which facilitates its fine dispersion in the polymer matrix, porous matrix or bioactive coating on the total hip prostheses. It exhibits excellent biocompatibility, bioactivity, bone-bonding and osteoconductive properties [50, 84].



Fig. 10 Hydroxyapatite.

Polymer/ceramic compositions were used as a bone cell supporting matrices due their biocompatibility and mechanical properties, which are indispensable for bone regeneration. However, the using of HAp in the biomedical application as a substrate to stimulate bone in-growth is limited due to its brittleness [85, 86].

2.2.3 Biodegradable Polymer/hydroxyapatite Composite

2.2.3.1 HAp/polymer Solution

In 2004, alloplastic materials for the treatment of odontogenically caused bone defect were studied. Copolymer based on poly(ethylene glycol) and poly(D,L-lactic-co-glycolic acid) was implanted into the bone defect in three different forms: powder, gel and gel with HAp. The most suitable form of material for application in bone defects is a combination of gel and powder in a weight proportion of 50:50) [87].

Lee et al. prepared PLGA/HAp composite films by solvent-casting method. PLGA powder with HAp (5, 10 and 15 wt %) was dissolved in chloroform. The solvent was evaporated overnight. The composites based film was placed into the incubator and chondrocyte were added. Enhance of cell attachment and proliferation on the surface of the film was observed [88].

In 2010 nanofibrous PLGA/gelatin/HAp were fabricated by an electrospinning method. PLGA and gelatin (in various ratios) were dissolved in hexafluoroisopropanol (HFIP) a then HAp nanoparticles (20% of total weight) were added. The nanofibrous composites improved mechanical properties, osteoconductivity and biocompatibility and may be used as scaffolds for bone tissue engineering [89].

2.2.3.2 Silanization of HAp-surface

Oliveira et al. in 2005 developed a hybrid material using γ -methacryloxypropyltrimethoxy-silane (γ -MPS) as a coupling agent between the organic (polymer) and inorganic phase (glass reinforced hydroxyapatite) registered as Bonelike. Hybrid materials when exposed to an aqueous physiological environment can lose strength rapidly at the inorganic-organic interface. Polymer phase was prepared using PLGA (with the molar ratio of D, L-lactide to glycolide equal to 85:15). Silanized or non-silanized discs of Bonelike were soaked in 1 - 20 wt % of PLGA polymer solution. Bonelike silanized surface acted as more effective coupling agent [90].

2.2.3.3 Synthesis of Core-shell Nanospheres

Xiangan et al. prepared core-shell nanospheres of hydroxyapatite/chitosan (HAp/CS) in multiple emulsions. In the preparation of HAp/CS core-shell nanospheres, the mixed solution of $\text{Ca}_2(\text{NO}_3)_2 \cdot 4\text{H}_2\text{O}$, chitosan and $(\text{NH}_4)_2\text{HPO}_4$ were used. Amino groups of the chitosan interacted with $-\text{OH}$ groups of the HAp nanospheres by hydrogen bonds to form a shell. This way of preparing inorganic/organic core-shell nanospheres have potential application in bone tissue recovery [91].

Experimental part of this thesis describes mainly characterization of viscoelastic properties of both unmodified and ITA or HAp modified PLGA—PEG—PLGA copolymer by test tube inverting method (TTIM) and dynamic rheological analysis. The next chapter briefly describes the introduction to rheology of polymers.

2.3 Polymer Rheology

The word “rheology” was coined by Prof Bingham in 1920s [92]. Rheology, a branch of mechanics, is the study of those properties of materials which determine their response to mechanical force. The measurement of rheological properties is applicable to all material types – from fluids to semi-solids and solid systems (e.g. polymer solution, polymer melts, composites). Properties of material are linked with their molecular structure and conditions (temperature) [93].

The polymeric systems often display very viscoelastic properties and they have a wide range of used. We find the polymer in every-day situation, whether in the human body such as blood proteins or in the nature resins and gums. This includes polymeric product that surround us every-day life - plastic articles or consumer product packing [92].

2.3.1 Polymeric Liquids

Polymeric liquids exhibit both liquid and solid like behavior. Their dynamic properties cannot be thermodynamic constants because they have dependence on the history of forces acting on it (e.g. shear rate or shear stress). Solution of high-molecular weight polymer already at low concentration can flow only slowly. Addition of a small amount of polymer into the solution, make the fluid very viscous. The primary motivation to study polymeric fluids (or polymeric liquids) comes from commercial and industrial application. Generally, properties of polymeric solution help to formulate a polymer system in respect to its processing characteristics [93].

2.3.2 Newtonian Fluids

Polymer solution (sol phase) displayed the characteristics of a *Newtonian fluid*. The viscosity of a Newtonian fluid is dependent only on temperature but not on shear rate and time. The response of a Newtonian fluid is characterized by a linear relationship between the applied shear stress (τ) and the shear rate ($\dot{\gamma}$) (1) [ref]:

$$\eta = \frac{\tau_{xy}}{\dot{\gamma}} \quad (Pa \cdot s) \quad (1)$$

where σ_{xy} is the shear stress $\dot{\gamma}$ is the shear rate.

For most the Newtonian fluids, the viscosity decreases with temperature and increases with pressure.

2.3.3 Non-Newtonian Fluids

Polymer melts or the most polymer solutions are among the *Non-Newtonian fluids*. The apparent viscosity is not constant but is a function of (shear stress) τ or (shear rate) $\dot{\gamma}$. The viscosity is not only a function of flow conditions, but also depends on the kinetic history of the fluid element under consideration.

Time independent fluids are characterized by the change of an apparent viscosity with changing shear rate. Depending on previous conditions, there are three possibilities: shear-thinning (pseudoplastic), viscoplastic behavior with or without shear-thinning behavior, shear-thickening (dilatant fluid) (Tab. 3). The fluids have no memory of their past history [94].

Table 3: Newtonian and Non-Newtonian fluid [95]

Newtonian fluid			<i>milk, water, mineral oil</i>
Non-Newtonian fluid	time dependent	thixotropic	<i>yogurt, paint</i>
		rheopectic	<i>gypsum paste</i>
	time independent	shear thinning	<i>slurries, shampoo</i>
		shear thickening	<i>wet sand, concentrated starch suspension</i>
		plastic	<i>tooth paste, grease</i>

The apparent viscosities in *time dependent fluids* are not function of the applied shear stress or the shear rate, but the viscosity of fluids change with the duration of shearing which are connected with previous kinematic history. This group includes thixotropic and rheopectic fluids [93]. Flows curves are showed in Fig. 11.

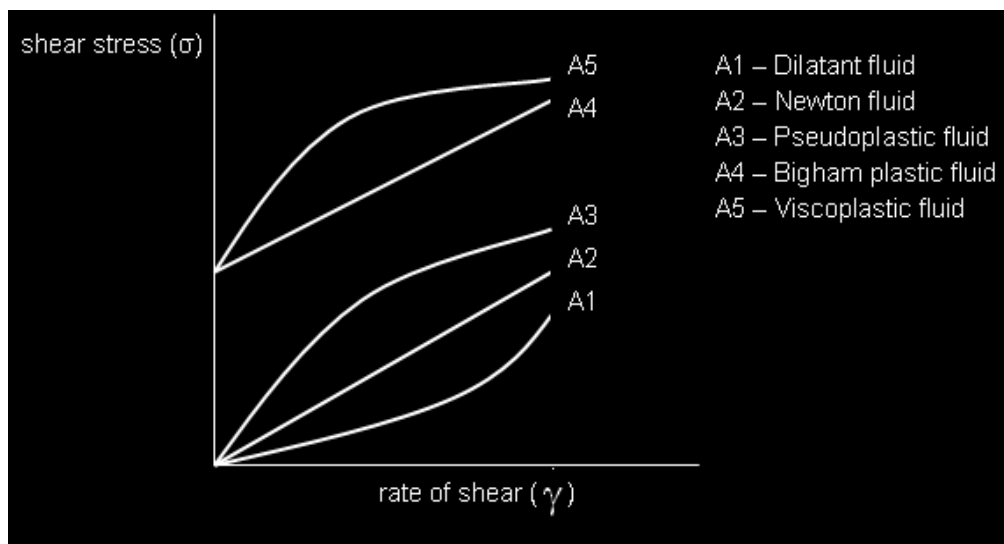


Fig. 11 Flow curves for different types of fluids.

2.3.4 Viscoelastic Behavior of Polymeric Solution

Rheological measurements are used for characterization of viscoelastic properties of polymeric melts or solutions. Viscoelastic properties are investigated using rheological experiments such as dynamic mechanical testing, which offers a convenient way to assess time or temperature dependence of mechanical properties of polymers [96].

Depending on the viscosity of testing material size or HAp of the geometry in dynamic rheological analysis can be selected. For measurements of very low viscosity (to medium viscosity) materials Concentric Cylinders geometry is used. Cone Plate geometry was found to be suitable for the measurement of low viscosity (to high viscosity or filled system with very small particles) and Parallel Plate geometry is in principle used for Soft Solid (or filled system with bigger particles than in Cone Plate) [97, 98] (Fig. 12).

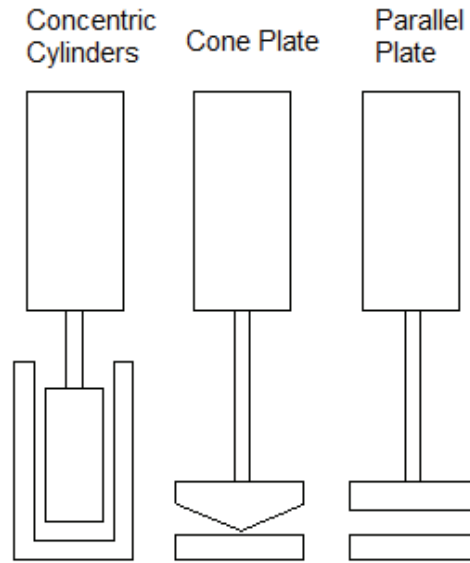


Fig. 12 The most commonly used geometry in dynamic rheological analysis.

2.3.4.1 Linear Viscoelastic Region

The method used for measuring linear viscoelastic response is *oscillatory testing*, i.e. applying an oscillating stress or strain as an *input* to the (co)polymer and monitoring the resulting oscillatory strain or stress *output*. Other method very often used is frequency sweep, time or temperature sweep [96].

Strain or Stress Sweep

If a sinusoidal stress (or strain), σ (force acting over an area) a sinusoidal displacement will result which is in phase with the applied stress (strain). The material response to increasing deformation amplitude (strain or stress) is monitored at constant frequency and temperature (Fig. 13).

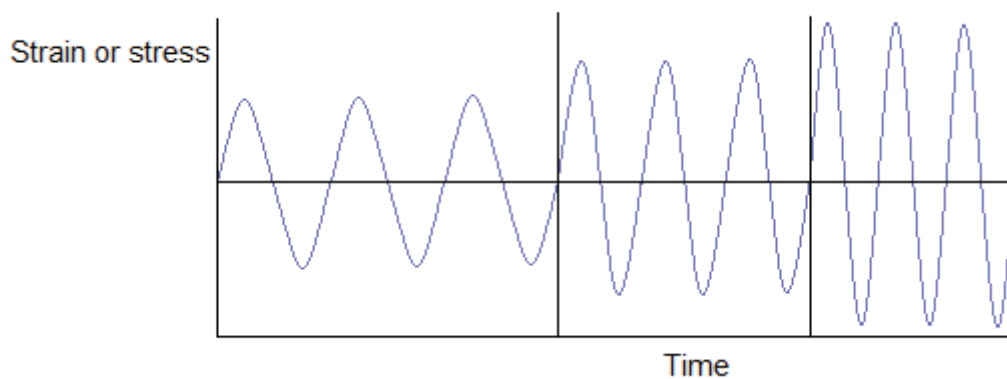


Fig. 13 Increasing value of sinusoidal amplitude (strain or stress).

Shear strain γ is represented via a sinusoidal form (2) [ref]:

$$\gamma = \gamma_0 \sin(\omega \cdot t) \tag{2}$$

where γ_0 is the strain oscillatory amplitude, ω = angular frequency and t is time.

However, the shear stress τ is also described with the sinusoidal amplitude with a phase angle (3) [ref]:

$$\tau = \tau_0 \sin (\omega \cdot t + \delta) \quad (3)$$

where τ_0 is stress oscillatory amplitude and δ is a phase angle.

Frequency Sweep

The constant strain (or stress) used in frequency sweep should be in linear region. The samples have to be stable. The frequency sweep changing time to complete of one oscillation (Fig. 14). For instance, the typical resting heart rate in adults is 60–80 bpm (beats per minute) whereas the children have heart rate up to 200 bpm. This number depends on the child's age [99].

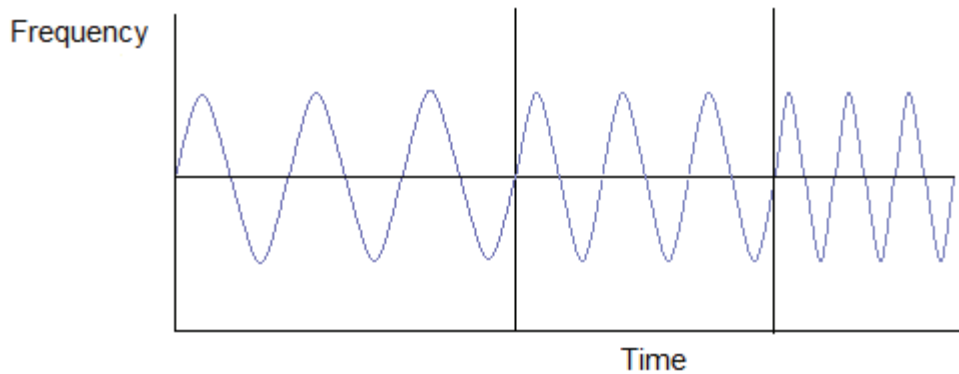


Fig. 14 Frequency sweep.

In frequency sweep are used two units - angular frequency (rad/s) or frequency (Hz). The relationship between them can be expressed as follows. One hertz (Hz) is equal to $6.28 \text{ rad}\cdot\text{s}^{-1}$.

2.3.4.2 Oscillatory Tests with a Maxwell Model

If we oscillate an ideal spring, all frequencies $G' = G$ the spring modulus and G'' is zero. On the other hand, when we oscillate a perfect dashpot, the loss modulus is given by $G'' = \eta \cdot \omega$ and the G' is zero. Viscoelasticity is a combination of these two cases. The response of the simplest combination of these two elements in series - the Maxwell model - gives a far more complex and interesting behavior over a range of test frequencies as show in Figure 15.

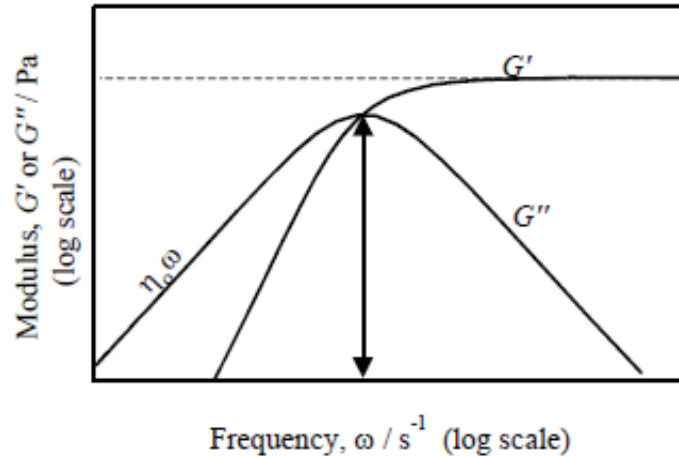


Fig. 15 Typical Maxwellian behavior in oscillatory testing, with the crossover point indicated [92].

Viscoelastic moduli are dependent on angular frequency which is given mathematically by equation (4). At very low frequencies, G'' is higher than G' and liquid-like behavior dominates. With increasing testing frequency, G' takes over and solid-like behavior prevails. The G'' is much more dependent on the angular frequency [92, 98].

$$G'' = \frac{\eta\omega}{1+(\omega\tau)^2} \quad \text{and} \quad G' = \frac{G(\omega\tau)^2}{1+(\omega\tau)^2} \quad (4)$$

In oscillatory testing, great care has to be taken to ensure that the experiment takes place in the linear region where G' and G'' are independent on the maximum amplitude of strain or stress of the oscillation and frequency. In the linear region G^* is constant, but in the non-linear region G^* is a function of shear rate ($\dot{\gamma}$) or angular frequency (ω) (Fig. 16) [95].

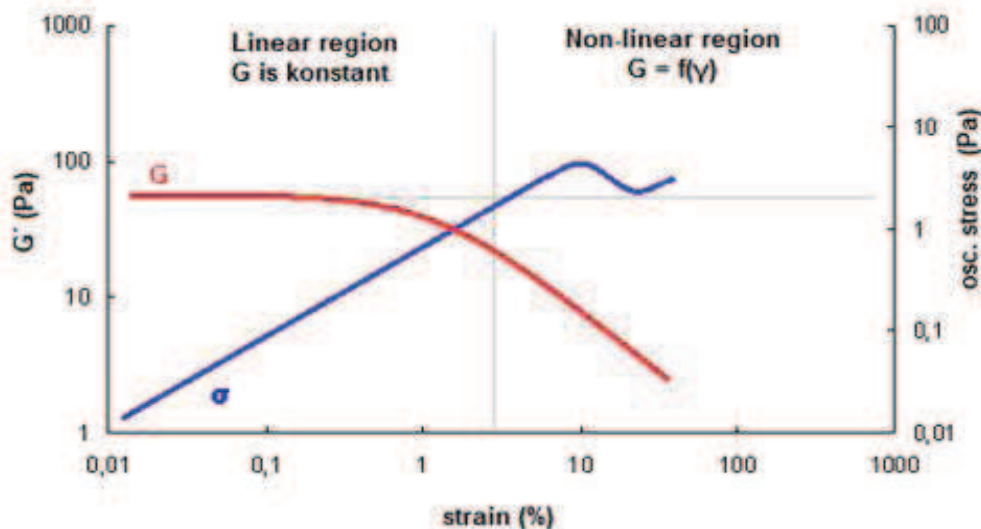


Fig. 16 Evaluation of G^* with the increasing value of shear rate.¹

Complex modulus measures of materials overall resistance to deformation. ¹ $G^* = G' + iG''$

The non-linear behavior of polymers can cause a local shear thickening proceeding or pronounce shear thinning. In the linear viscoelastic range a Maxwell model, corresponding to a single relaxation time and an elastic plateau modulus, generally describes dynamic moduli [92].

In 1968, Winter and Chambond presented viscoelastic phenomenon of the crosslinking polymers. Measurements were performed on polydimethylsiloxane (PDMS) model networks. The study described viscoelastic behavior of a crosslinking polymer near the gel point. In their theory the gel point were determined as $G' = G''$ a crossover that depends on the angular frequency (Fig. 17) [100].

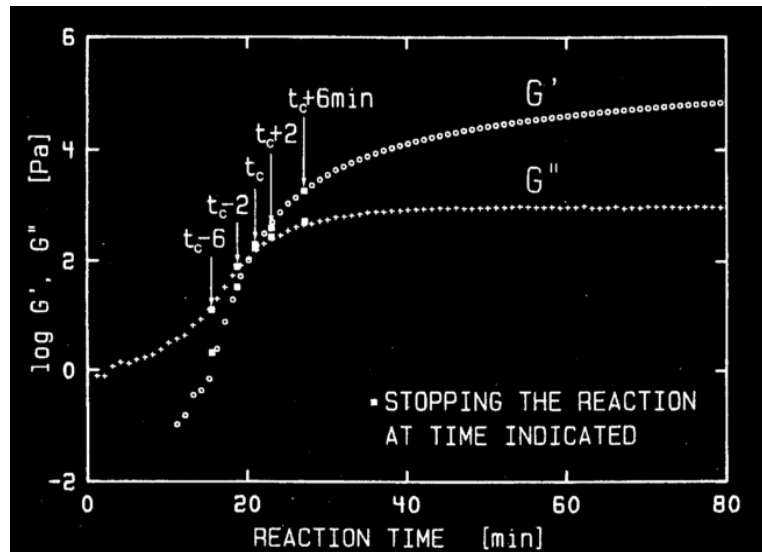


Fig. 17 Evaluation of the storage modulus G' and the loss modulus G'' of a crosslinking polymers.

2.3.5 Gelation Behavior of PLGA—PEG—PLGA

The gelation behavior of aqueous solution of commercial PLGA—PEG—PLGA named ReGel[®] was characterized by rheological measurement and by test tube inverting method. However, it was investigated degradation rate which depends strongly on the temperature. ReGel[®] fills important drug delivery duration of 1–6 weeks ReGel[®] and was selected as a suitable material for controlled drug delivery or candidate for intratumoral injectable material [101].

2.4 Goal of the Work

The main goal of the diploma work is to observe changes in viscoelastic properties of the original PLGA—PEG—PLGA copolymer, which gels at body temperature, in comparison with those, modified by the ITA or HAp and deciding whether or not would be the new polymeric material suitable as injectable drug carrier or bone adhesive in medical applications.

3 EXPERIMENTAL PART

3.1 Chemicals

- PEG ($M_n = 1\,500\text{ g}\cdot\text{mol}^{-1}$) and Sn (II)2-ethylhexanoate (95 %) were purchased from Sigma-Aldrich (Germany).
- D,L-lactide (LA, 99.9%) and glycolide (GA, 99.9%) were supplied from Polysciences (Pennsylvania, USA).
- Itaconic anhydride (ITA 97 %) were obtained from FLUKA (Switzerland) and sublimated prior the use.
- Ultrapure water (ultrapure water of type II according to ISO 3696) was prepared on Millipore Elix 5 UV Water Purification System (Millipore, Merck spol. s r. o.).
- Phosphate buffer saline with pH = 7.48 and phosphate buffer saline with pH = 9.00 were prepared using KCl, KH_2PO_4 , NaCl and Na_2HPO_4 , where pH was adjusted by HCl ($c = 1\text{ mol}\cdot\text{dm}^{-3}$) and NaOH ($c = 1\text{ mol}\cdot\text{dm}^{-3}$).
- Hydroxyapatite was purchased from Reicke

3.2 Equipments

- Rheometer AR-G2 (TA Instruments)
- Millipore (Elix 5)
- Micropipette (Laborgeräte Hirschmann)
- Laboratory freeze dryer (2-4 Alpha LSC Christ)
- pH Meter (S2K712, IsfetCom)
- Thermoblock (HLC TK 23, BioTech)
- Gel Permeation Chromatography (Agilent Technologies 1100 Series)
- Analytical scale (Mettler Toledo)
- Laser Particle Size Analyser (ANALYSETTE 22 Microtec plus, Fritsch)
- Scanning electron microscope (ZEISS EVO LS 10 with EDS-detector) (SEM)
- Proton Nuclear Magnetic Resonance (500 MHz NMR spectrometer Bruker AVANCE III, Masaryk University)

3.3 Methods

3.3.1 Synthesis of PLGA—PEG—PLGA Copolymer

The PLGA—PEG—PLGA triblock copolymers with weight ratio of PLGA/PEG equal to 2.0 or 2.5 and molar ratio of LA/GA equal to 3.0 were synthesized via ring opening polymerization method in a bulk under nitrogen atmosphere as described elsewhere [47]. Briefly, PEG ($M_n = 1500$, 2.3 mmol) was degassed and dewatered at 130 °C for 3 h under the vacuum and D,L-lactide (48 mmol) and glycolide (16 mmol) monomers were added against the nitrogen outflow. After the homogenization by stirring, Sn(II)2-ethylhexanoate (0.22 mmol) as organic catalyst was injected in order to start up the copolymerization at 130 °C.

3.3.2 Preparation of ITA/PLGA—PEG—PLGA/ITA Copolymer

Functionalization of the PLGA—PEG—PLGA triblock copolymer proceeded with sublimated ITA (2.5 molar ratio to polymer) at 110 °C for 2 hours in “one pot” reaction (see Fig. 6).

3.3.3 Samples Purification

The obtained crude copolymer was purified by three purifying agents PBS (pH = 7.48 or 9) and ultrapure water. After being completely dissolved, the polymer solution was heated to 80 °C to precipitate the polymer product and remove water-soluble low-MW polymers and unreacted monomers. The purification process was repeated 3x times. The residual water in the precipitated copolymer was frozen at -18 °C over night and lyophilized at -70 °C in freeze dryer until the constant weight.

3.3.4 Preparation of Copolymer Water Solution

The homogenous polymer solution with a given concentration was prepared by dissolving the polymer in 1 mL of ultrapure water and stirred in cold water bath (4 – 8 °C). The time of complete dissolving is depended on the hydrophobic/hydrophilic ratio (PLGA/PEG). After being completely dissolved, the polymer solution was used to test tube inverting (TTIM) method and for rheological properties characterization.

3.3.5 Preparation of PLGA—PEG—PLGA/HAp Composites

Hydroxyapatite was mixed directly into the sol phase at laboratory temperature. The mixture was stirred until became homogenous and after that was kept at 4 °C.

3.4 Characterization

3.4.1 Scanning Electron Microscope (SEM)

For surface characterization of microstructure of HAp scanning electron microscope ZEISS EVO LS 10 with EDS-detector was used. The specimens of powder were performed on the carbon tape and coated with gold before examination. Accelerating voltage (10 and 5 kV) and working distance (7.5 and 8.5 mm) were used.

3.4.2 Laser Particle Size Analyser

The particle size distribution and mean particle size were measured using laser particle size analyser ANALYSETTE 22 Microtec plus. Distilled water was employed as the dispersion medium and small amount of HAp powder was added into the wet dispersion unit.

3.4.3 Proton Nuclear Magnetic Resonance (^1H NMR)

Molecular weight and ITA functionalization were evaluated using proton nuclear magnetic resonance (^1H NMR) spectroscopy on 500 MHz Bruker AVANCE III instrument using 128 scans in CDCl_3 solvent.

3.4.4 Gel Permeation Chromatography (GPC)

Number-average molecular weight (M_n) and polydispersity index (M_w/M_n) of the copolymers were measured using gel permeation chromatography (GPC) method using Agilent Technologies 1100 Series instrument equipped with isocratic pump, autosampler, RI and UV-VIS detector, fraction collector, guard column 50×4.6 mm and column 250×4.6 mm both PLgel $3 \mu\text{m}$ MiniMIX-E thermostated up to 80°C with THF as the eluent at a flow rate of $0.1 \text{ mL}\cdot\text{min}^{-1}$ against linear polystyrene standards.

3.4.5 Test Tube Inverting Method (TTIM)

The test tube inverting method (TTIM) was used to determinate the sol-gel phase transition temperature. The vials containing polymer solutions were immersed in a thermoblock at designated temperature for 7 min (Fig. 18) Condition of flow (sol phase) or no flow (gel phase) were observed by inverting a vial vertically. The sample was regarded as a “gel” in the case of no visual flow within 30 s by inverting the vial with a temperature increment of 1°C per step.



Fig. 18 Thermoblock used for test tube inverting method.

3.4.6 Dynamic Rheological Analysis

The sol-gel transition and other rheological properties of the copolymer aqueous solution was investigated in a dynamic stress-controlled rheometer with Cone Plate geometry (angle 2° , diameter 40 mm and gap $60\ \mu\text{m}$). Cold polymer solution ($600\ \mu\text{L}$) was transferred to the Peltier (temperature control system) by micropipette. Rheometer was prepared to the working position. Before each measurement the solvent trap was filled with distilled water and the liquids were used to prevent evaporation of the sample (Fig. 19).

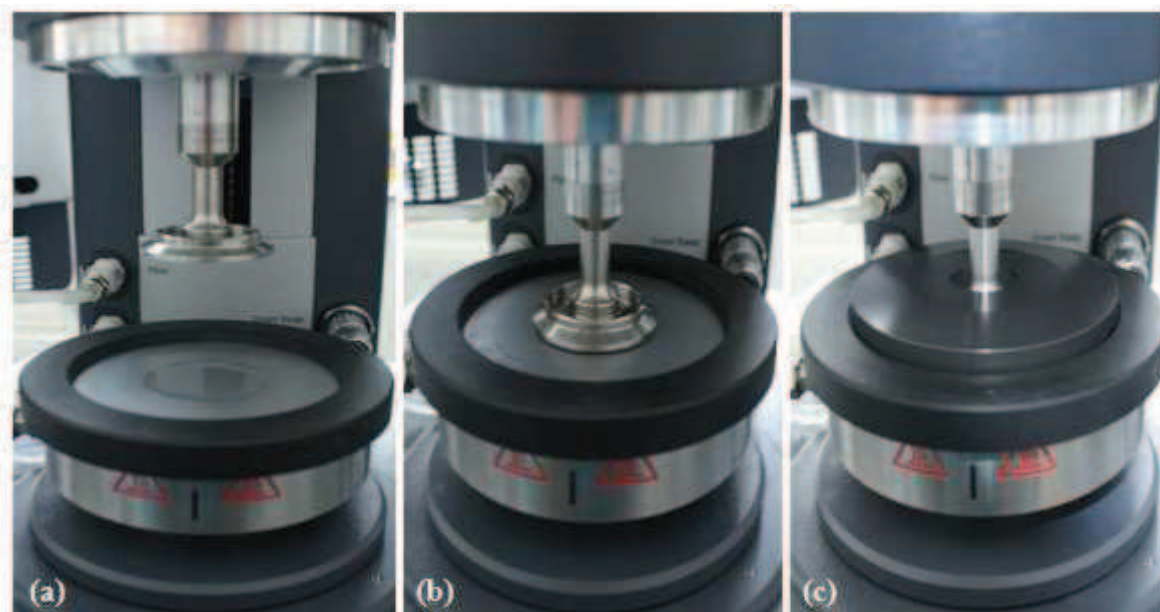


Fig. 19 (a) adding cold polymer solution (b) working position (c) lid was used to prevent evaporation of the sample.

Experiments were carried out at constant angular frequency of $1\ \text{rad}\cdot\text{s}^{-1}$ with temperature ramp from 15 to $60\ ^\circ\text{C}$ and a rate of $0.5\ ^\circ\text{C}\cdot\text{min}^{-1}$. The temperature delay time was set to $30\ \text{sec}$ and stress was fixed at $0.4\ \text{Pa}$.

4 RESULTS AND DISCUSSION

The main idea of the research is preparation of polymer composites based on heterogeneous core/shell submicron-sized particles dispersed in a thermogelling aqueous sol of degradable polymeric matrix (e.g. PLGA—PEG—PLGA). The inorganic core (e.g. hydroxyapatite) of submicron-sized particles might be coated by degradable multifunctional copolymer from renewable resources (e.g. ITA/PLGA—PEG—PLGA/ITA). Copolymer modified by ITA can be cross-linked either chemically by covalent bonding through the double bonds (e.g. via photopolymerization) and/or physically (by hydrogen bonds or ionic interactions with Ca^{2+} cations from HAp) in order to produce new functionalized 3D-hydrogel network. After being crosslinked, core-shell microspheres could be mixed with thermogelling PLGA—PEG—PLGA solution in order to achieve prolonged and controlled hydroxyapatite release in bone fixing, healing or regeneration.

However, main aim of the proposed diploma work was synthesis, characterization and rheological study of thermogelling polymers based on the PLGA—PEG—PLGA either functionalized with ITA or modified with HAp. The effect of ITA or HAp modification on thermogelling properties of original PLGA—PEG—PLGA copolymer has been evaluated and is discussed below.

4.1 Characterization of Copolymers

Based on previous experiences of our group, ITA was used to functionalize PLGA—PEG—PLGA copolymer with PLGA/PEG weight ratio equal to 2.0 and LA/GA molar ratio of 3.0 (A and B samples), while HAp was mixed with the PLGA—PEG—PLGA copolymer having same LA/GA molar ratio but PLGA/PEG weight ratio equal to 2.5 (A1 sample). When synthesized, unmodified and ITA or HAp modified PLGA—PEG—PLGA copolymers were characterized in the term of chemical structure by gel permeation chromatography (GPC) and proton nuclear magnetic resonance (^1H NMR). GPC was used to determinate number-average molecular weight and polydispersity index (M_w/M_n) of both PLGA—PEG—PLGA (A; A1) and ITA/PLGA—PEG—PLGA/ITA (B) copolymers. PLGA/PEG weight ratio, LA/GA molar ratio and molecular weights were determined by ^1H NMR spectroscopy from integrals of characteristic proton intensities as described elsewhere [47]. Molecular weight's properties and chemical compositions of prepared copolymers are shown in Tab. 4. It can be seen that results obtained by both GPC and NMR are in very good agreement with theoretical prediction.

Table 4: Chemical properties of prepared copolymers.

Polymer Sample	M_w/M_n^a	PLGA/PEG ^c (wt %)	PLGA/PEG ^b (wt %)	LA/GA ^c (mol %)	LA/GA ^b (mol %)	M_n^a	M_n^b	M_n^c
						(kg·mol ⁻¹)		
A*	1.20	2.0	N.A.	3.0	N.A.	6.19	N.A.	4.50
A1	1.21	2.5	2.16	3.0	2.44	6.78	4.74	5.25
B	1.20	2.0	2.04	3.0	2.84	5.56	4.56	4.50

^a measurement by GPC, ^b results obtained from ^1H NMR, ^c theoretical calculation

sample A and A1: copolymer PLGA—PEG—PLGA, sample B: copolymer ITA/PLGA—PEG—PLGA/ITA

* Prepared PLGA-PEG-PLGA polymer was divided into two parts. One part of unmodified ABA polymer is labeled as sample A whereas second part was additionally modified by ITA labeled as sample B. The presence of the ITA was verified by ^1H NMR method, thus sample A was characterized only by GPC.

4.1 Characterization of HAp Particles

HAp powder used for polymer/HAp composites was characterized by scanning electron microscope and laser particle size analyser. A scanning electron microscope was used to analyze the microstructure of HAp powder. For observation, low acceleration voltage of 10 kV (Fig. 20 A) or 5 kV (Fig. 20 B) and short working distance (7.5 or 8.5 mm) was used, respectively. The picture (A) shows particles with diameter at around 6 - 7 μm . Higher magnification of surface depicts more details of non-spherical particles.

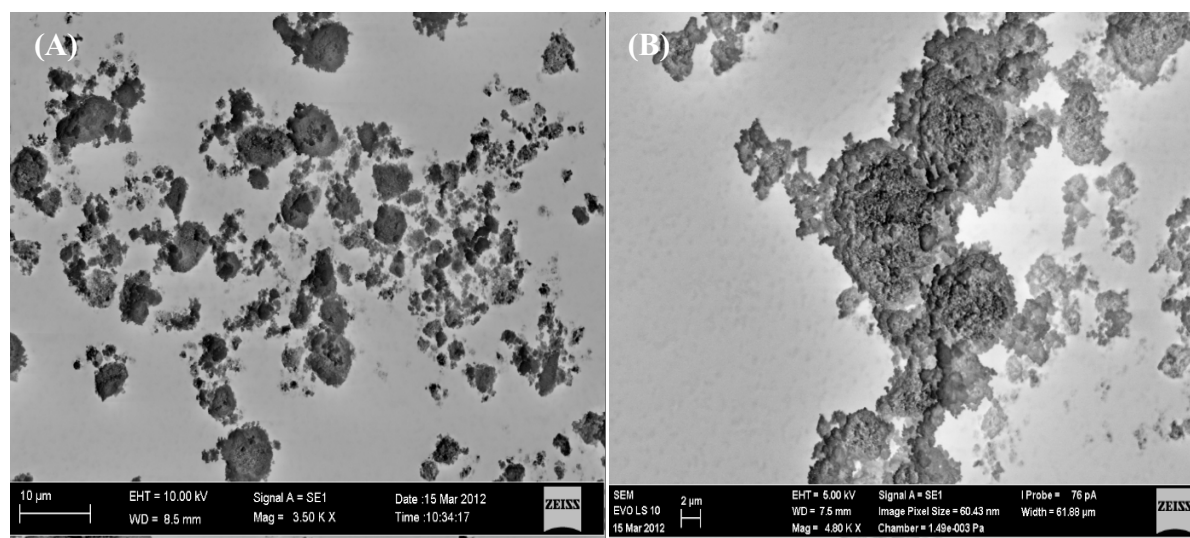


Fig. 20 SEM micrographs of the HAp powder.

The size of particulate HAp powder was as well characterized using laser particle size analyser. Fig. 21 shows particle size range from 1 to 26 μm . Distribution curve exhibits monomodal distribution. The mode/mean of particles size was determined on 6.32 and 7.00 μm .

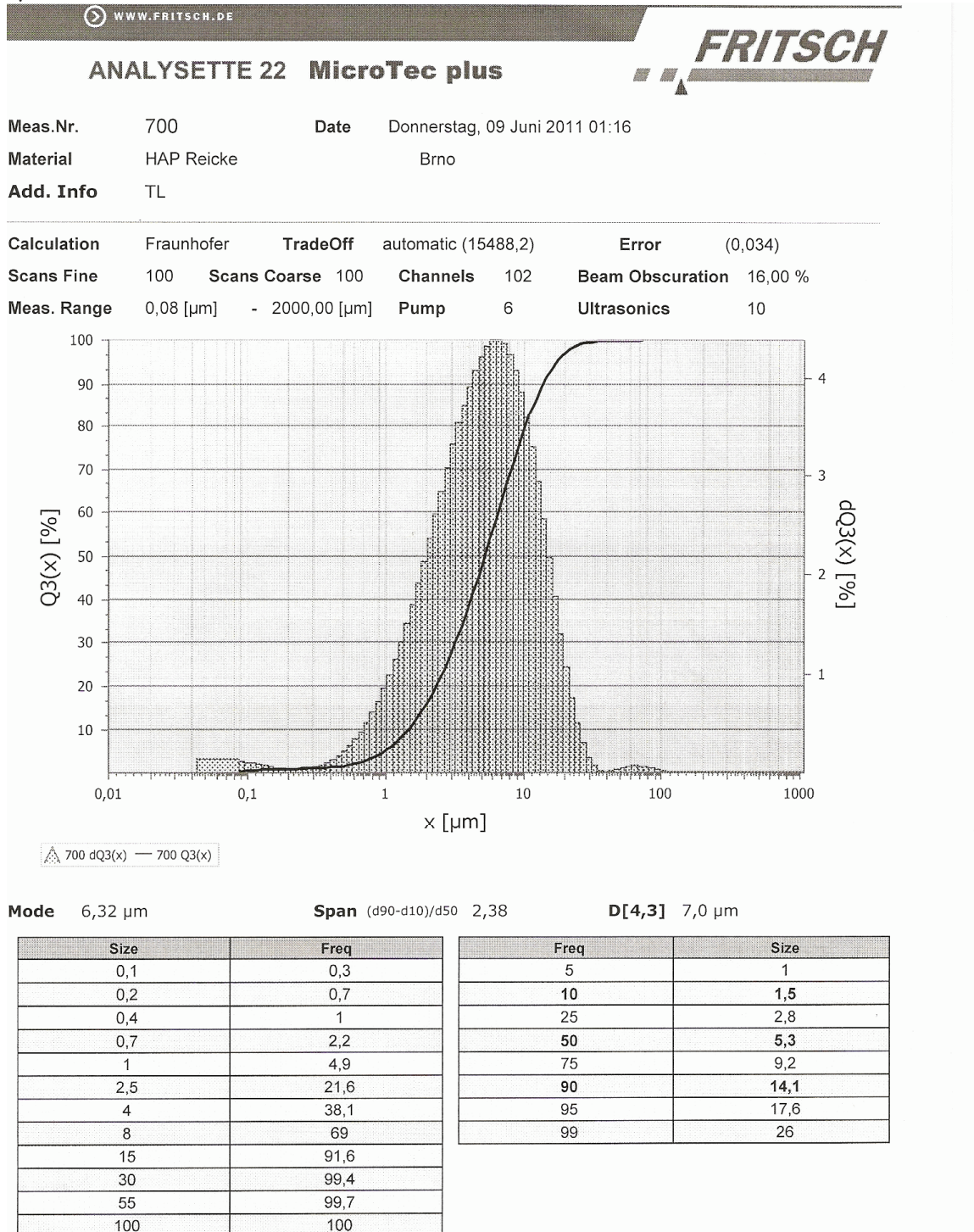


Fig. 21 Particle size analysis of HAp powder.

4.2 Gel Point Determination

The thermosensitive triblock copolymers are soluble in water at low temperature and when the temperature increases above the critical gelation temperature the physical hydrogel is formed. The sol-gel and gel-suspension transition of unmodified PLGA—PEG—PLGA copolymers and ITA or HAp modified copolymers were observed by both test tube inverting method (TTIM) and rheological analysis with a view to compare determined gel points.

4.2.1 Test Tube Inverting Method

The test tube inverting method (TTIM) was used to determinate the sol-gel phase transition temperature. Advantage of TTIM is sol-gel visualization with determination of the critical gelation concentration (CGC) and critical gelation temperature (CGT). All changes (viscosity, solubility and color) observed by test tube inverting method describes phase transition diagram. The typical phase diagram of a polymer solution concentration is a function of temperature showing three regions – sol, gel and suspension.

Focusing on the 22 wt % concentration of PLGA—PEG—PLGA (sample A1) at temperature much lower than critical gelation temperature, the solution behaves as transparent sol (20 °C). The first sol-gel transition has appeared at 22 °C followed by transparent gel up to 25 °C at which the gel turned to turbid gel. The turbid gel turned to white gel at 32 °C. The copolymer exhibited the second phase transition from white gel to suspension at 41 °C after which the polymer was precipitated from the water (see Fig. 22).

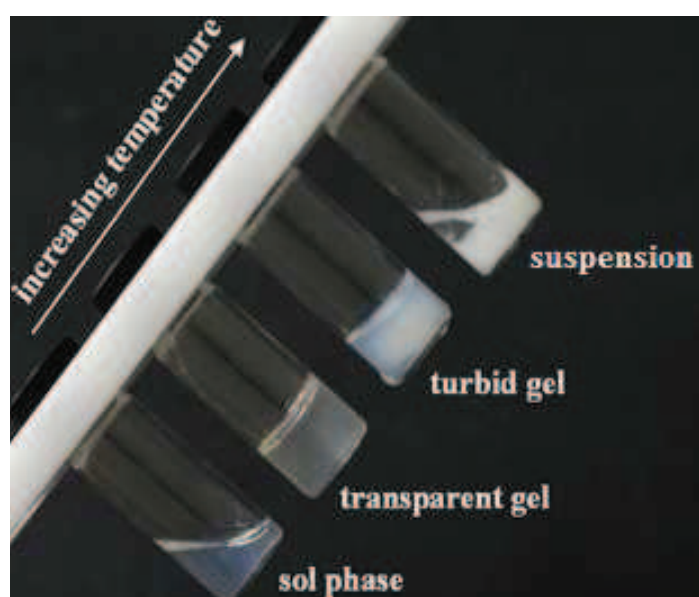


Fig. 22 Evaluation of gel with increasing temperature for PLGA—PEG—PLGA triblock copolymer ($c = 22$ wt %).

4.2.1.1 PLGA—PEG—PLGA Copolymers

Fig. 23 and 24 shows sol-gel phase transition diagrams of A and A1 samples prepared according to TTIM data, where “gel phase” is divided into transparent, turbid and white gel. The critical gelation temperature (CGT) and critical gelation concentration (CGC) of PLGA—PEG—PLGA triblock copolymers with PLGA/PEG ratio of 2.0 and 2.5 (sample A

and A1, respectively) were determined. While sample A exhibited CGT equal to 39 °C and CGC of 14 wt %, sample A1 showed CGT at 30 °C keeping same CGC as sample A. When compared A and A1, the higher the PLGA/PEG ratio the lower CGT was obtained. Both diagram curves demonstrated that with increasing polymer concentration the gelation temperature decreased.

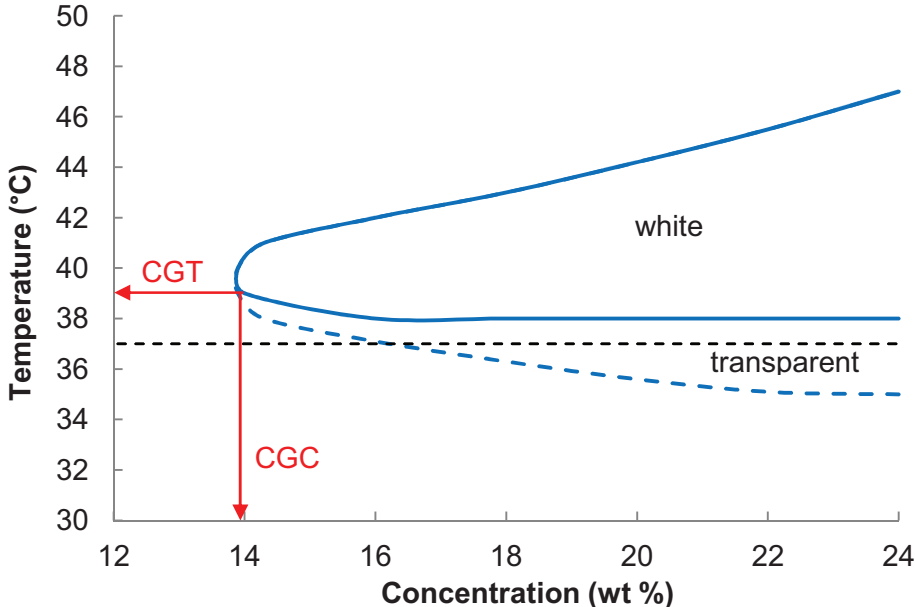


Fig. 23 Phase transition diagram of PLGA—PEG—PLGA triblock copolymer (sample A).

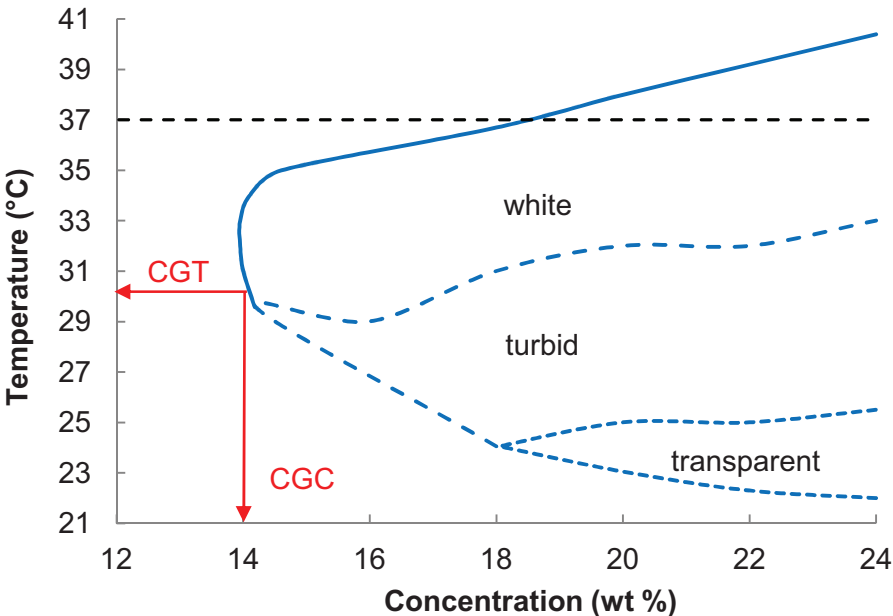


Fig. 24 Phase transition diagram of PLGA—PEG—PLGA triblock copolymer (sample A1).

4.2.1.2 ITA/PLGA—PEG—PLGA/ITA Copolymer

The CGT and CGC of ITA/PLGA—PEG—PLGA/ITA triblock copolymers water solutions of 6 – 24 % concentration were determined as 33 °C and 10 wt %, respectively (see Fig. 25). ITA modification (sample B) causes the decreasing in critical gelation concentration of sample A (from 14 to 10 wt %) for the current decrease in critical gelation temperature (from 39 to 33 °C). The ITA functionalized copolymer gels earlier (at lower temperature) probably due to the contribution of new ionic interactions of –COOH bonds within a physical gel. As discussed later in the thesis, the ITA modified hydrogel was even more stiff in comparison to hydrogel from unmodified PLGA—PEG—PLGA copolymer.

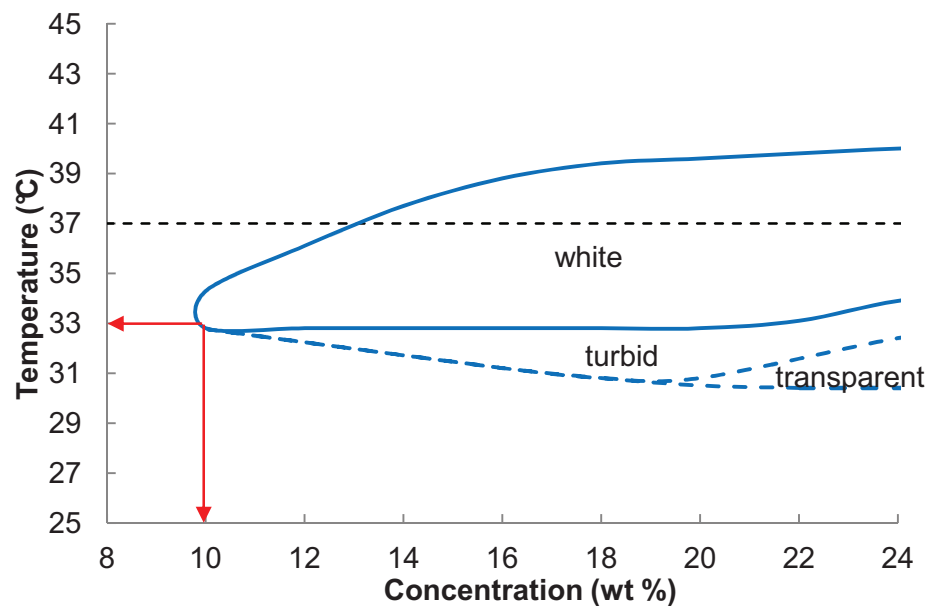


Fig. 25 Phase transition diagram of ITA/PLGA—PEG—PLGA/ITA (sample B).

4.2.1.3 PLGA—PEG—PLGA/HAp Composite

HAp microparticles were mixed directly with PLGA—PEG—PLGA water solution and prepared copolymer/HAp composite rheological properties were evaluated using TTIM. During gelation process the system did not go from low viscosity liquid via high viscosity liquid towards to hard viscoelastic solid, but goes from the low viscosity to hard viscoelastic gel. Copolymer with adding amount of HAp exhibited liquid-like behavior up to 32 °C observing the gel already at 33 °C. It can be caused by rapid increase in gel stiffness due to HAp modification where ionic interactions took place.

4.2.2 Dynamic Rheological Analysis

Rheological measurements of unmodified and ITA or HAp modified triblock copolymers bring accurate temperature of phase transitions, maximum values of G' , G'' , $\tan \delta$ (G'/G'') and complex viscosity. The linear region of dynamic rheological analysis was evaluated by stress and frequency sweep measurement.

4.2.2.1 Linear Region

During temperature sweeping, stress amplitude was set at the appropriate value determined from pre-test to achieve linearity of viscoelasticity. The dynamic viscoelastic functions such as the dynamic shear storage modulus (G') and loss modulus (G'') were measured as a function of angular frequency, temperature and stress.

4.2.2.2 Stress Sweep

The experiments were carried out using a controlled stress rheometer. The rheological behaviors of polymer samples were monitored with the changing stress amplitude (0.1-100 Pa) at constant frequency ($1 \text{ rad}\cdot\text{s}^{-1}$) and temperature (37°C). The values of stress amplitude were checked to ensure that all measurements were carried out within viscoelastic region. For the oscillation testing (stress sweep) the PLGA—PEG—PLGA water solution having concentration of 22 wt % was prepared. The sample was weakly dependent on the oscillatory stress (see Fig. 26).

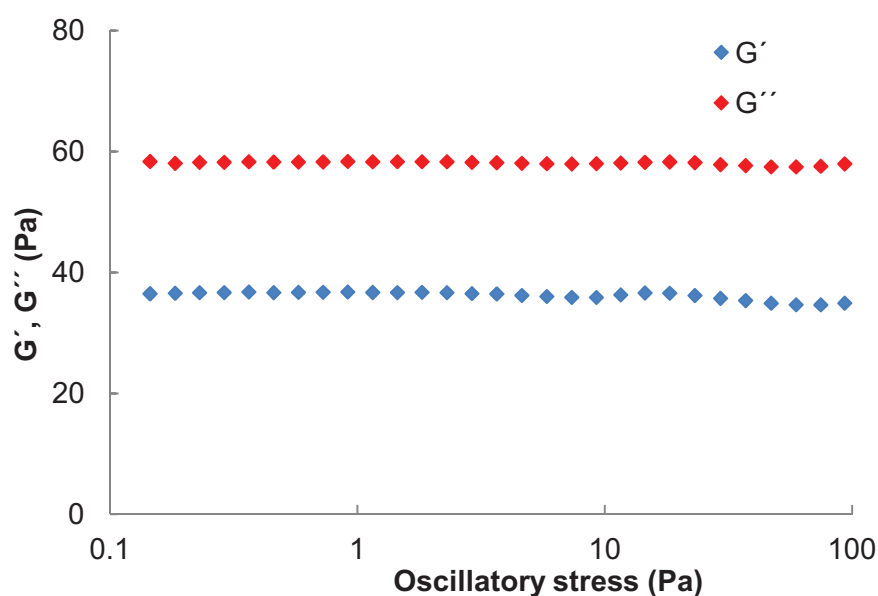


Fig. 26 Dynamic moduli of sample A1 ($c = 22 \text{ wt } \%$) at a fixed frequency of $1.0 \text{ rad}\cdot\text{s}^{-1}$ and temperature 37°C .

As for the oscillatory testing of polymer/HAp composite sample A1 ($c = 22 \text{ wt } \%$) containing 20 wt % HAp was prepared. The measurements showed that sample having higher degree of elasticity was strongly dependent on the oscillatory stress. (Fig. 27)

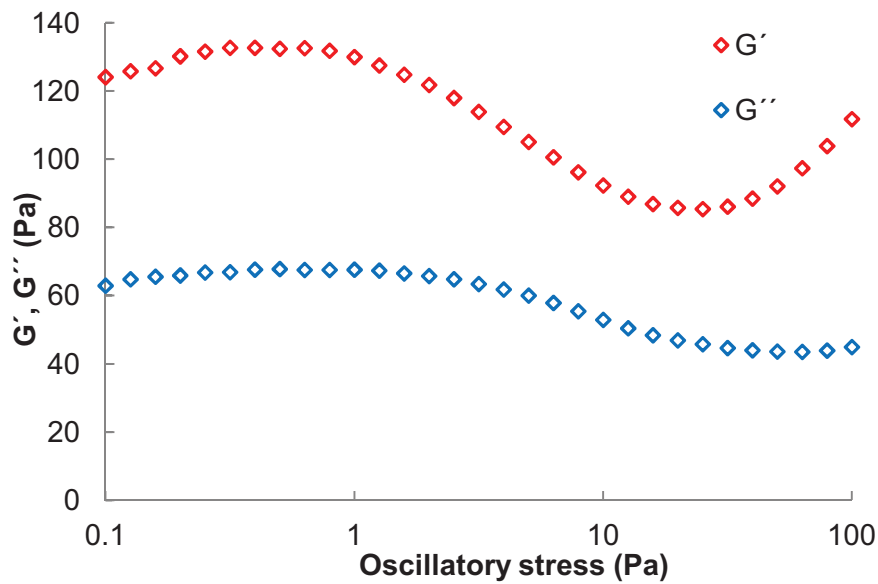


Fig. 27 Dynamic moduli (polymer concentration $c = 22$ wt %) at a fixed frequency of $1.0 \text{ rad}\cdot\text{s}^{-1}$ and temperature 37°C for sample with Hap.

This linear viscoelastic range is defined by constant dynamic moduli G' and G'' . For all measurements oscillatory stress of 0.4 Pa was selected as a range in which is no or infinitesimal evidence of changing in dynamic moduli.

4.2.2.3 Frequency Sweep

Polymeric solution of sample A1 ($c = 22$ wt %) was prepared with/without adding HAp to determine the linear viscoelastic region where the values of the moduli are independent of the applied frequency. The experiments were performed at constant temperature of 37°C and frequency range between $0.0628 - 62.8 \text{ rad}\cdot\text{s}^{-1}$ ($0.1 - 10 \text{ Hz}$). Both G' and G'' exponentially grows with the frequency except the low values (see Fig. 28).

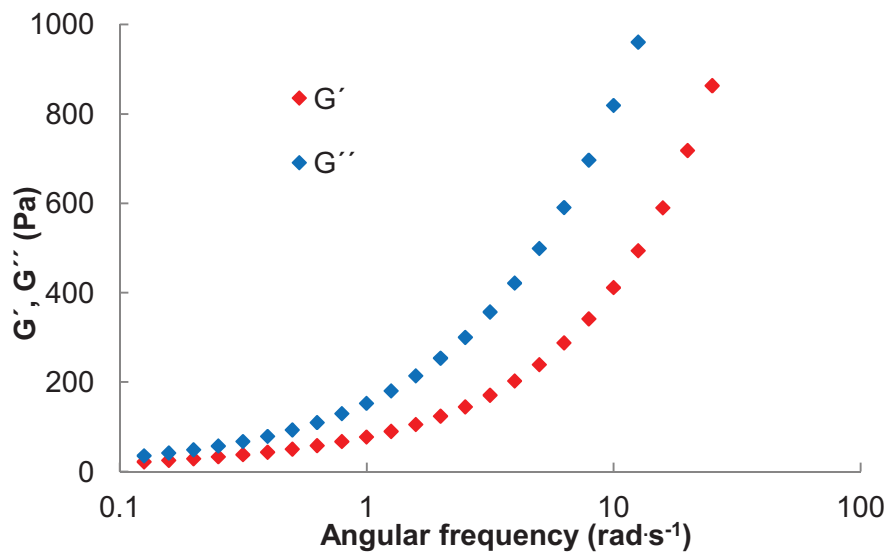


Fig. 28 Dynamic moduli of sample A1 ($c = 22$ wt %) at 37 °C and fixed oscillatory stress at 0.4 Pa.

Sample A1 (modified with 20 wt % of HAp) shows elastic dominant behavior in whole select frequency range. (see Fig. 29).

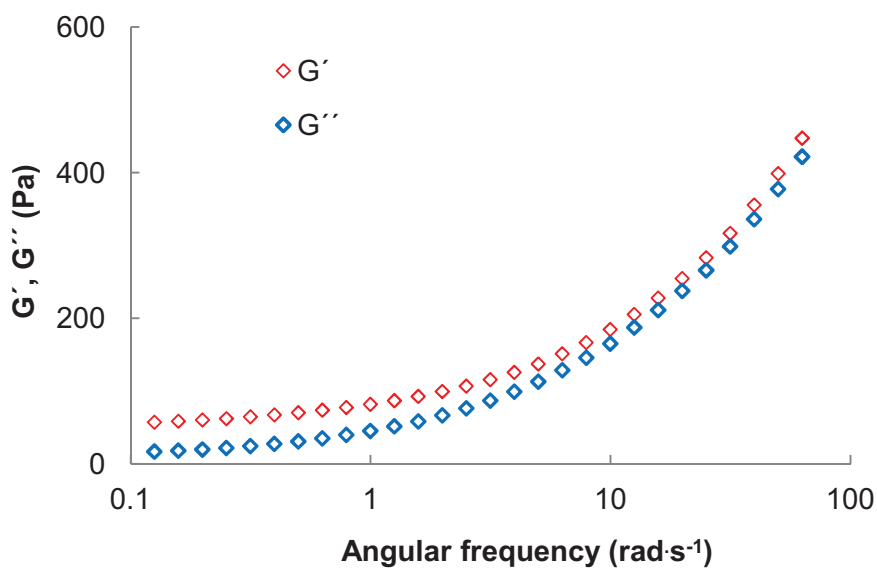


Fig. 29 Dynamic moduli of sample A1 ($c = 22$ wt %) with 20 % of HAp at 37 °C and fixed oscillatory stress at 0.4 Pa.

For the other experiments, frequency was set on the 1 rad·s⁻¹ in which is no evidence of intersection G' and G'' .

4.2.3 PLGA—PEG—PLGA Copolymers

4.2.3.1 Influence of Purifying Agents

The PLGA—PEG—PLGA copolymer purified via different agents (ultrapure water, PBS 7.48 and PBS 9) might exhibit significantly different physical behaviors. After purifying, the precipitated and dried sample A was further dissolved in cold ultrapure water (4 °C). Changes in viscoelastic properties were measured by dynamical rheological experiments (Fig. 30).

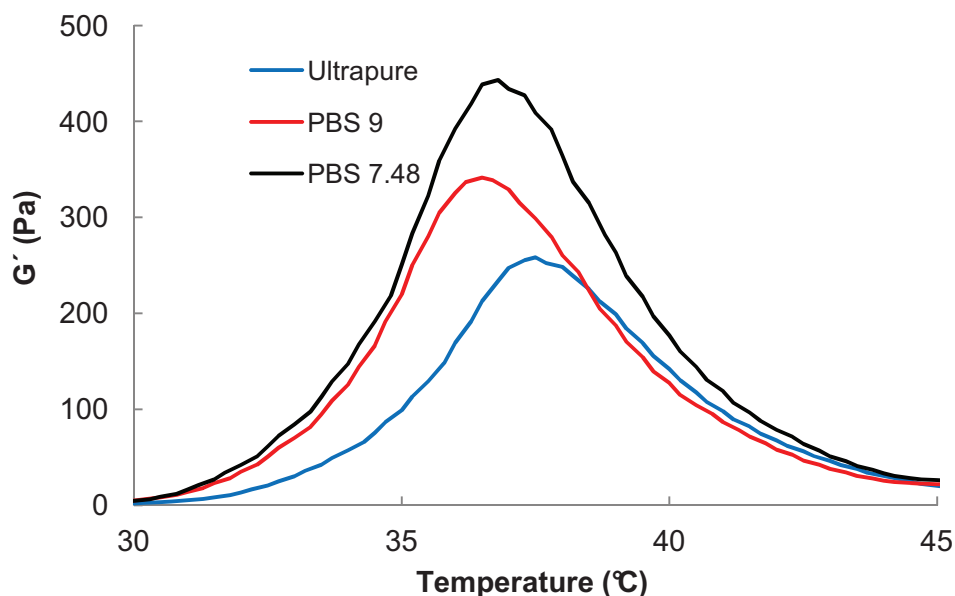


Fig. 30 Storage modulus G' of sample A (18 wt %) purified via ultrapure water, PBS 9 and PBS 7.48.

The maximum value of gel stiffness (443 Pa) exhibited copolymer purified via PBS 7.48, the lower gel stiffness (258 Pa) showed copolymer purified in PBS 9 and the copolymer purified in ultrapure water exhibited almost half value of gel stiffness (258 Pa) compared to G'_{\max} in PBS 7.48. As a results, purifying agents significantly changed the gel stiffness and the temperature of G'_{\max} values. Copolymer dissolved in PBS 7.48 or 9 exhibits higher value of G'_{\max} . It may be explained by polymer-solvent ionic interaction.

Rheological properties of series of PLGA—PEG—PLGA thermogelling copolymers (sample A and A1) with different concentrations (6 – 26 %) were studied in ultrapure water. The viscosity, gel stiffness (elasticity) and the range of applicability grow with the increasing polymer concentration (Fig. 31). It is evident, that higher PLGA/PEG ratio not only decreased the G'_{\max} but very significantly increased the gel stiffness (666 vs. 93 Pa).

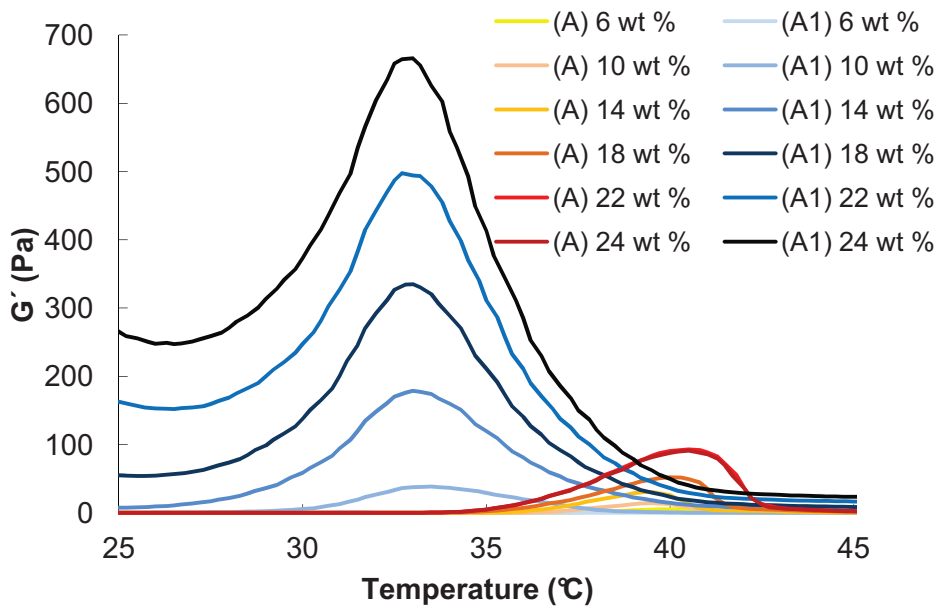


Fig. 31 Evolution of elastic modulus (G') of different concentration of PLGA—PEG—PLGA solution in ultrapure water – sample A1 (PLGA/PEG = 2.5) and sample A (PLGA/PEG = 2.0).

Copolymers show sol-gel (first transition) and gel-suspension transition (second transition). The sol-gel phase transition of PLGA—PEG—PLGA triblock copolymers was observed by both TTIM and rheological analysis. In rheology the gelation temperature can be defined by the first intersection of G' and G'' (1) (Fig. 32) and in the case of TTIM this temperature was noted determined when no visual flow of polymer within 30 s was observed.

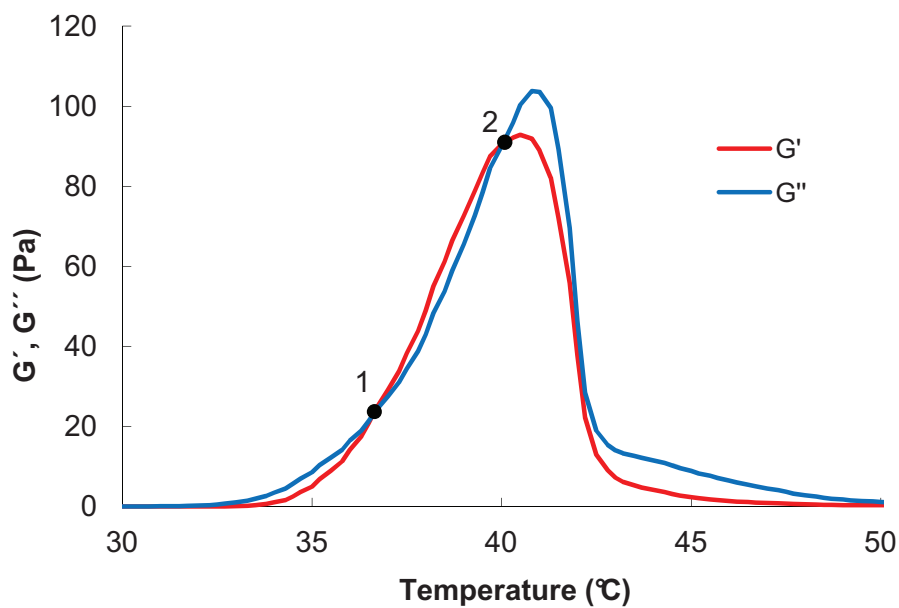


Fig. 32 Rheological measurement of sample A water solution ($c = 24$ wt %), where (1) is sol-gel transition and (2) is gel-suspension transition.

Second intersection of $G' = G''$ (Fig. 32 second cross-point) at 40 °C (A) or 34.5 °C (A1) ($c = 24 \%$) found via rheological measurement corresponding with gel-suspension transition. It should be attributed to the collapse of elastic gel, which relates with the rapid decrease of G' that falls below G'' forming suspension without viscoelastic behavior. Thermogelling behaviors were determined by TTIM and rheology (Fig. 33). It is evident, that maximum stiffness (G'_{max}) exhibited white gel (not clear one) and that the change between the transparent and white gel very well corresponded with the temperature of $\tan \delta$ minimum. This process is not a phase transition but only bigger size of compacting micelles turned the clear gel to the more stiff white one.

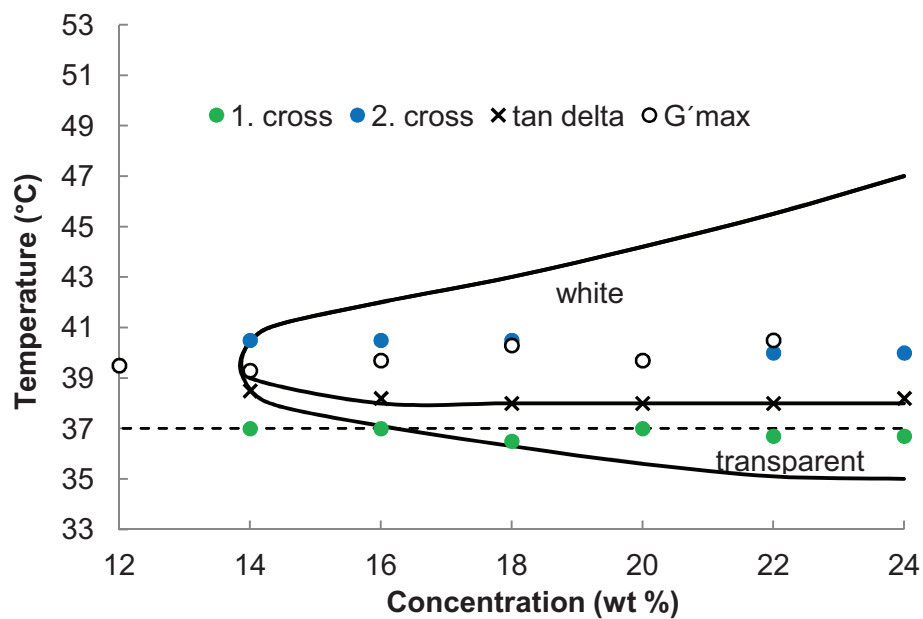


Fig. 33 Thermogelling behaviors by TTIM and rheology of different concentration of PLGA—PEG—PLGA solution in ultrapure water – sample A (PLGA/PEG = 2.0).

The accurate temperature of precipitation the polymer from water was detected by rheometer, because it is very difficult to establish loss of elastic properties of gel visually using TTIM. The gelation temperatures of sample A1 are compared in Table 5.

Table 5: Comparison of cross-points noticed by TTIM and rheological analysis

Polymer concentration (wt %)	TTIM		Rheology		pH	gel color
	1.cross	2.cross	1.cross	2.cross		
6	-	-	30.5	32.5	3.5	-
8	-	-	29.2	37	3.4	-
10	-	-	26.8	37	3.4	-
12	-	-	26.5	36	3.3	-
14	29	35	25.8	35.5	3.2	turbid
16	25	35	25.8	35.5	3.2	turbid

Polymer concentration (wt %)	TTIM		Rheology		pH	gel color
	1.cross	2.cross	1.cross	2.cross		
18	24	36	25.5	35.2	3.2	transparent
20	23	38	25.5	34.7	3.1	transparent
22	22	39	25.3	34.5	3.1	transparent
24	22	43	gel*	34.5	3.1	transparent

gel* - the sample was already a gel before measurement (high polymer concentration), thus the first cross point is missing.

4.2.4 ITA/PLGA–PEG–PLGA/ITA Copolymer

The gel point of newly synthesized thermosensitive ITA/PLGA–PEG–PLGA/ITA copolymer was characterized by both test tube inverting method (TTIM) and rheometer. The preliminary experiments showed that weight ratio PLGA/PEG = 2.0 and molar ratio of LA/GA = 3.0 is appropriate for ITA modification. Rheological properties of series of ITA/PLGA–PEG–PLGA/ITA copolymers with different concentrations (6 – 24 wt %) were studied in ultrapure water. The gel stiffness and the range of applicability grow with the increasing polymer concentration by moving the first gel point of copolymer to the lower temperature and maximum G' to body temperature (37 °C) (see Fig. 34).

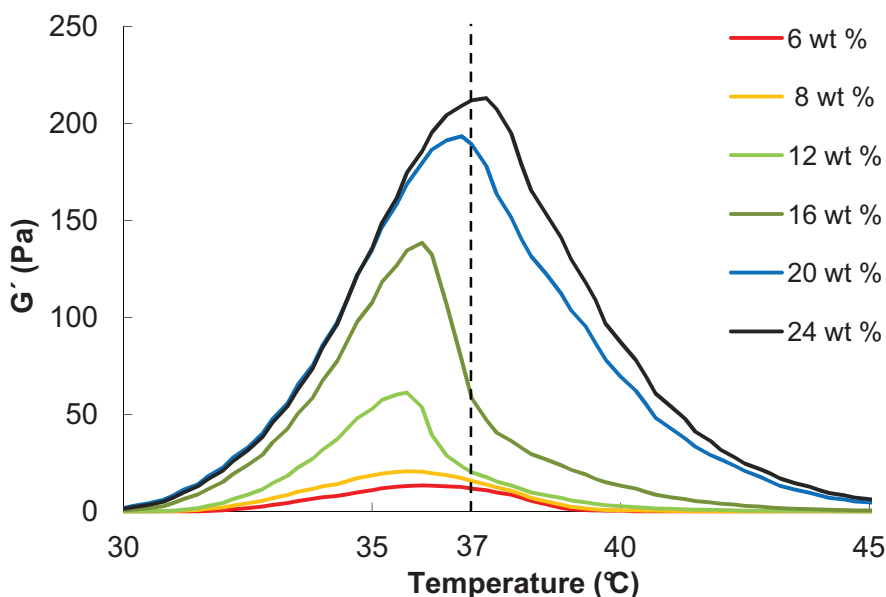


Fig. 34 Elastic modulus of ITA/PLGA–PEG–PLGA/ITA (sample B) at different concentration in ultrapure water.

Where compared thermogelling behaviors of sample B obtained by TTIM or rheometer, it can be seen that G'_{\max} belongs to the white gel stiffness and fluctuates around 37 °C. In that case, the $\tan \delta$ minimum corresponds very well with the situation where the turbid gel changes to the more stiff white gel – as similarly described at sample A (see Fig. 35).

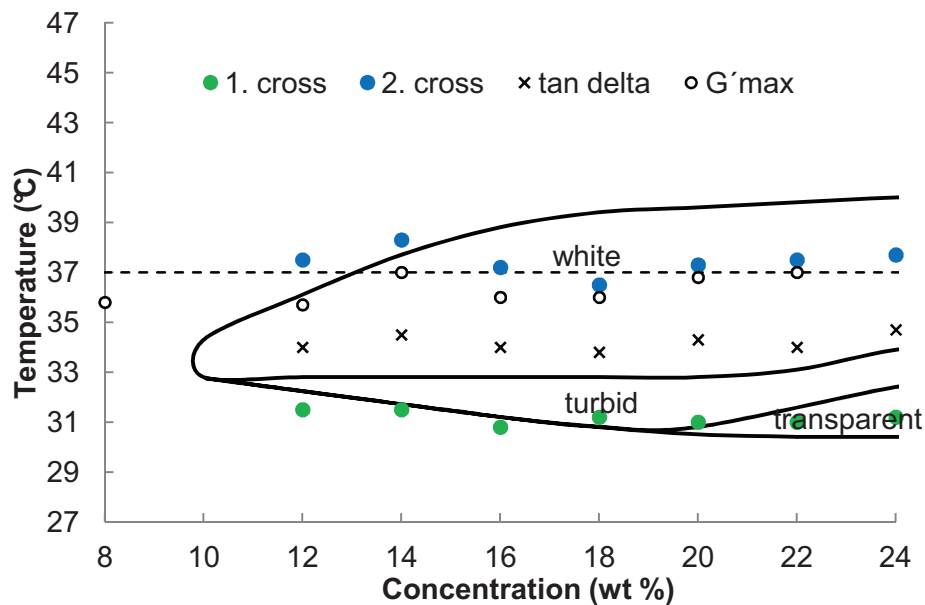


Fig. 35 Thermogelling behavior by TTIM and rheology of different concentration of ITA/PLGA—PEG—PLG/ITA solution in ultrapure water – sample B (PLGA/PEG = 2.0).

In comparison, the unmodified PLGA—PEG—PLGA copolymer exhibited two times lower max. values of G' than the ITA modified copolymer (e.g. 93 Pa vs. 203 Pa for 22 wt % concentration) (see Fig. 36). Unmodified copolymer shows the first cross point at higher temperature (36.7 °C, at $c = 22\%$) while ITA modified copolymer starts to gel at lower temperature (31.2 °C) but loss viscoelastic properties earlier (37.5 °C vs. 40 °C). The observed effects can be explained by ionic interaction of carboxyl-terminated sample B. In table 6 there are summarized elastic moduli for both copolymers detected by rheometer.

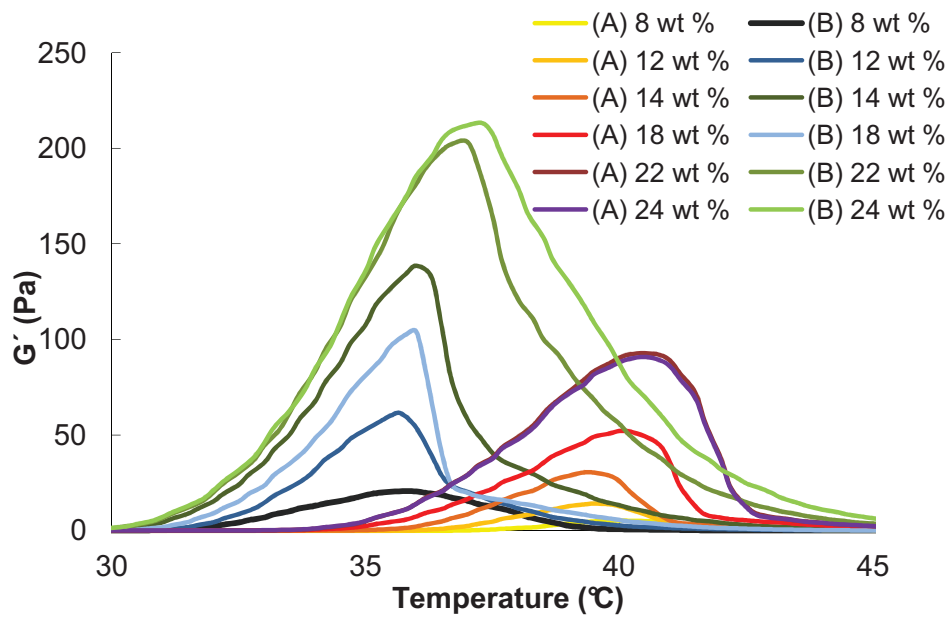


Fig. 36 Evolution of elastic modulus (G') of different concentration of PLGA—PEG—PLGA solution in ultra pure water – sample A (PLGA/PEG = 2.0) and sample B (PLGA/PEG = 2.5).

Table 6: Viscoelastic properties of PLGA—PEG—PLGA (Sample A) and ITA/PLGA—PEG—PLGA/ITA (Sample B) copolymers solutions with $c = 22$ wt %

	G' (Pa)	G' ($^{\circ}$ C)	1. cross ($^{\circ}$ C)	2. cross ($^{\circ}$ C)
Sample A	93	40.5	36.7	40
Sample B	203	37	31.2	37.5

4.2.5 PLGA—PEG—PLGA/HAp Composites

Polymer water solutions of sample A1 (concentration 10, 18 and 22 wt %) were mixed with HAp powder (0, 10, 20, 30, 40, 50 wt %). Figure 37 shows elastic modulus as a function of temperature and adding amount of HAp for 10 wt % of polymer. HAp modification changed the original rheological properties of sample A1 significantly.

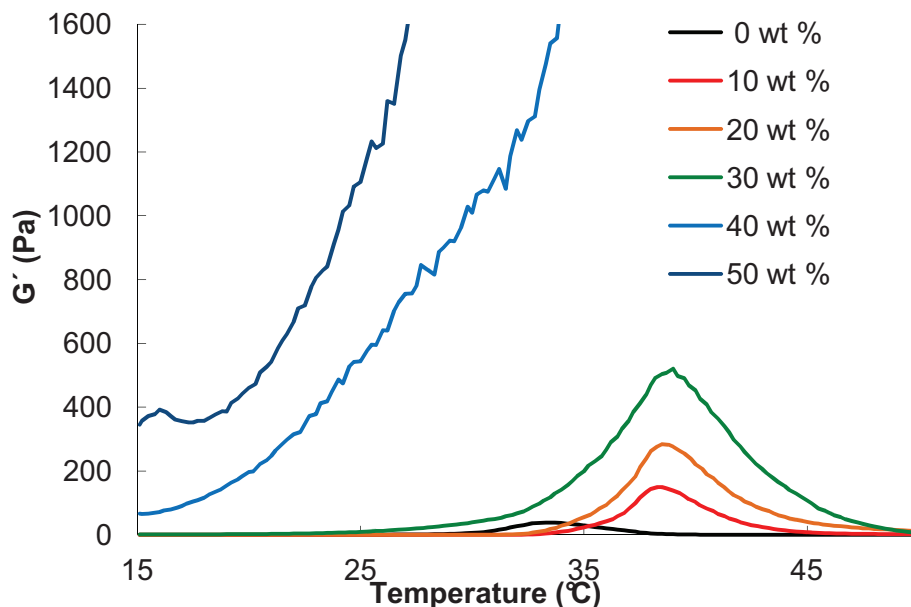


Fig. 37 Elastic modulus (G') as a function of temperature and adding amount of HAp-powder, $c = 10$ wt % of PLGA—PEG—PLGA in ultrapure water.

All samples showed increasing in gel stiffness after adding HAp. The values of G'_{\max} of sample A1 polymer solution ($c = 10$ wt %) increased from 11.9 Pa (at 33.5 °C) up to 7 204 Pa (at 39 °C) by adding 50 wt % of HAp to the PLGA—PEG—PLGA copolymer.

In comparison of 10 and 22 wt %, higher polymer concentration exhibited much higher gel stiffness with HAp addition. While unmodified PLGA—PEG—PLGA copolymers of 10 and 22 wt % have max. values of G' at 33.5 °C equal to 12 Pa and at 32.7 °C equal to 497 Pa, respectively, after adding 50 wt% of HAp the value of G'_{\max} moved to the higher temperature (39 and 36.7 °C) and much higher stiffness (7204 and 86 200 Pa), respectively. All rheological measurements are summarized in table 7.

Table 7: Changing of G' and pH with adding amount of HAp.

adding of HAp	polymer solution $c = 10$ wt %			polymer solution $c = 22$ wt %		
	G'_{\max} (Pa)	G'_{\max} (°C)	pH	G' (Pa)	G'_{\max} (°C)	pH
0 wt%	11.9	33.5	3.4	497	32.7	3.1
10 wt %	82	38.3	6.1	1 170	37.5	5.6
20 wt %	159.4	38.5	6.2	1 574	37.3	5.8
30 wt %	358	39	6.2	1 698	37.3	5.9
40 wt %	2 554	38.7	6.2	6 456	37.5	6.1
50 wt %	7 204	39	6.3	86 200	36.7	6.1

Figure 38 shows dependence of elastic modulus (G') on the amount of HAp powder in semi-logarithmic moduli axe plot for 10, 18 and 22 wt % concentration of sample A1. As can be seen, the gel stiffness grows significantly with increasing polymer concentration and added amount of HAp. Higher gel stiffness may be caused by strong ionic interaction between —OH groups of both HAp and copolymer. In all cases, elastic moduli increases very slowly up to 30 wt % content of HAp, but higher addition of HAp (40 or 50 wt %) exhibited much higher elastic moduli but very rough curves. Samples with 40 and 50 wt % of HAP were as well more viscous in sol state and high amount of HAP in gel state probably distorted the measurement where the gel is too stiff and very solid.

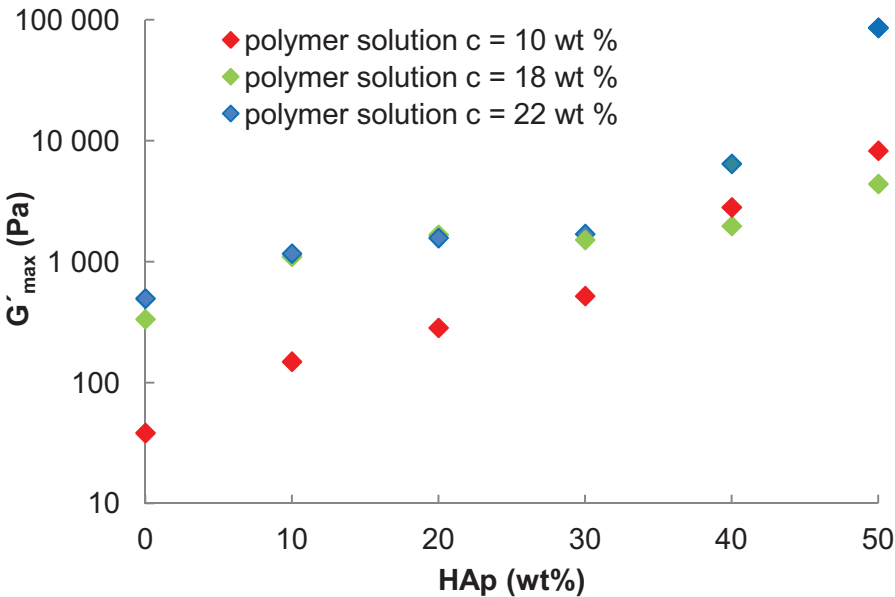


Fig. 38 Dependence of elastic moduli on adding amount of HAp-powder.

As can be seen in Fig. 39, in all cases the temperature of max. values of G' increased of about 5 °C after HAp addition, even at low HAp concentrations (e.g. from 32.7 °C up to 37.5 – 38 °C at $c = 22$ wt %). Finally, the optimal polymer concentration for HAp modification is 18 wt %, since HAp addition increase the temperature of G'_{max} very close to body temperature (37 °C).

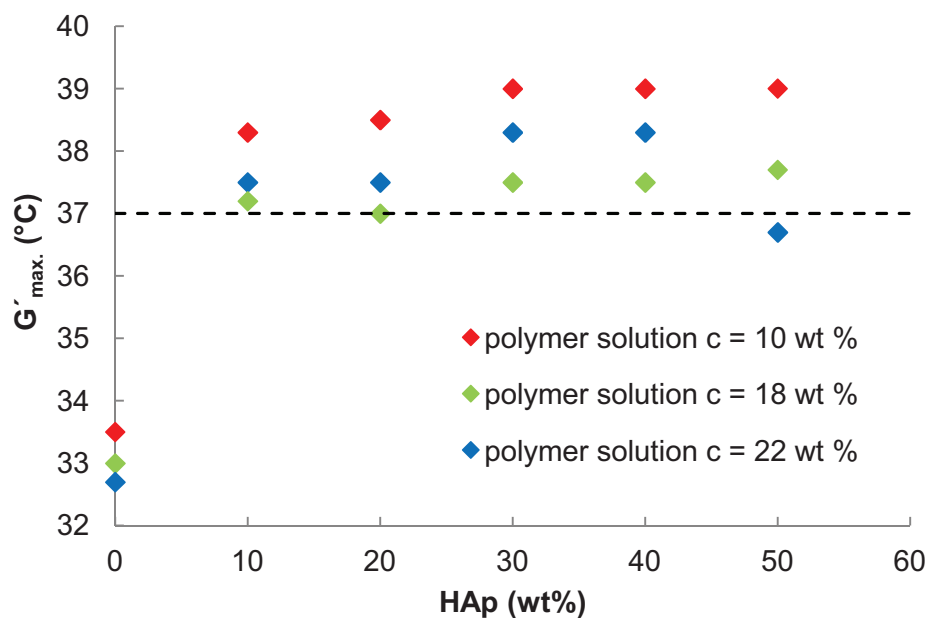


Fig. 39 Influence of added amount of HAp (wt%) on the temperature of maximum gel stiffness (G'_{max}).

5 CONCLUSION

The aim of presented work was to evaluate rheological properties of thermosensitive PLGA—PEG—PLGA copolymers functionalized by ITA or HAp by both test tube inverting method (TTIM) and dynamic rheological analysis. Prepared copolymers' water solutions (6 -24 wt %) exhibited sol-gel transitions induced by increasing temperature.

As for unmodified PLGA—PEG—PLGA copolymer, the CGT decreased (from 39 to 33 °C) with PLGA/PEG weight ratio increasing (from 2.0 to 2.5), whereas the CGC remained 14 wt %. The polymer having PLGA/PEG equal to 2.5 exhibited much higher gel stiffness (666 Pa) than polymer with PLGA/PEG = 2.0 (93 Pa) probably due to the much stronger hydrophobic interactions between longer PLGA polymer ends. The storage (elastic) modulus G' increased proportionately with higher polymer concentration. Purifying the polymer by PBS at pH = 7.4 increased the gel stiffness almost two times comparing to ultra pure water purification because of newly formed ionic interactions.

ITA functionalization of PLGA—PEG—PLGA increased G'_{\max} (from 93 to 203 Pa, $c = 24$ wt %) and moved the G'_{\max} temperature closer to body temperature (from 40.5 to 37.3 °C) in comparison with unmodified copolymer due to the new strong ionic interactions of —COOH groups.

When HAp was added to PLGA—PEG—PLGA water solutions, gelation of the polymer composites started later at the temperature higher of about 5 °C and closer to 37 °C, whereas the gel stiffness increased significantly (from 497 up to 86 200 Pa for polymer of $c = 22$ wt % and HAp = 50 wt %) and pH was moved from acidic (3.1) to more neutral (6.3) values.

In conclusion, both TTIM and dynamic rheological measurement helped us to better understand the thermogelling process of modified biodegradable PLGA—PEG—PLGA copolymers. Either ITA functionalization or HAp modification increased the gel stiffness of original unmodified PLGA—PEG—PLGA while approaching the temperature of G'_{\max} to body temperature, which makes them suitable as injectable hydrogels for drug delivery or bone regenerative medicine, respectively.

6 REFERENCES

1. Ratner, B. D.; Hoffman, A. S.; Schoen, F. J.; Lemons. J.: *Biomaterials Science. An Introduction in Medicine*. Biomaterials Science. Elsevier, Academic Press, 2a Edition. 2004
2. Gunatillake, P., A.; Adhikari, R.: *Biodegradable synthetic polymers for tissue engineering*. European Cells and Materials. 2003, vol. 5, p. 1–16. ISSN 1473–2262
3. Rahaman, M. N.; Day. D. E.; Bal, B. S.; Fu. Q.; Jung. S. B.; Bonewald. L. F.; Tomsia, A. P.: Bioactive glass in tissue engineering. *Acta Biomaterialia*. 2011, vol. 7, pp. 2355–2373
4. Azevedo H. S.; Reis, R. L.: Understanding the Enzymatic Degradation of Biodegradable Polymers and Strategies to Control Their Degradation Rate. *Biodegradable Systems in Tissue Engineering and Regenerative Medicine*. 2004. pp. 178–180
5. Mayer, M. H.; Hollinger, J. O.: *Biodegradable bone fixation devices*. In: *Biomedical Applications of Synthetic Biodegradable Polymers*. Hollinger J.O, ed. CRC Press, Boca Raton, FL. pp. 173-195
6. Abe, A.; Dušek, K.; Kobayashi, S.: *Biopolymers: Lignin, Proteins, Bioactive Nanocomposite*. Advances in Polymer Science. 2010. ISBN 978-3-642-13629-0
7. Middleton, J., C.; Tipton, A., J.: *Synthetic biodegradable polymers as orthopaedic devices*. *Biomaterials*. 2000, vol. 21. pp. 2335–2346
8. Burg, K., J., L.; Porter, S.; Kellam, J., F.: Biomaterial developments for bone tissue engineering. *Biomaterials*. 2000, vol. 21., pp. 2347–2359
9. Eschbach, L.: Nonresorbable polymers in bone surgery. *Injury, Int J care Injured*. 2000, vol. 31, pp. D22-D27
10. Ramakrishna, S.; Huang, Z.-M.; Kumar G. V.; Batchelor, A. W.; Mayer, J.: *An Introduction to Biocomposites: Series on Biomaterials and Bioengineering*. 2004 by Imperial College Press, vol. 1.
11. Kandziora, F.; Bail, H.; Schmidmaier, G.; Schollmeier, G.; Scholz. M.; Knispel, C.; Hiller, T.; Pflugmacher, R.; Mittlmeier, T.; Raschke, M.; Haas, N, P.: *Bone morphogenic protein-2 application by a poly(D,L-lactide)-coated interbody cage: in vivo results of a new carrier for growth factors*. *Journal neurosurg*. 2002. vol. 109, pp.1580-1584

12. Toung, J. S.; Ogle, R. C.; Morgan, R. F.; Lindsey, W. H.: Repair of rodent nasal critical-size osseous defect with osteoblast augmented collagen gel. *Laryngoscope*. 1999. vol. 109, pp. 277-288
13. Olsen, D.; Yang, C.; Bodo, M.; Chang, R.; Leigh, S.; Baez, J.; Carmichael, D.; et al.: Recombinant collagen and gelatin for drug delivery. *Adv. Drug Deliv Rev.* 2005. vol. 55, pp. 1547-1567
14. Aper, T.; Schmodt, A.; Duchrow, M.; Bruch, H. P.: Autologous blood vessels engineering from peripheral blood sample. *Eur. J. Vas. Endovasc. Surg.* 2007. vol. 33, pp. 33-39
15. Ehrbar, M.; Metters, A.; Zammaretti, P.; Hubbell, J. A.; Zisch, A. H.: Endothelial cell proliferation and progenitor maturation by fibrin-bound VEGF variants differential susceptibilities to local cellular activity. *J. Control. Release.* 2002. vol. 101, pp. 93-109
16. Nishinari, K.; Takahashi, R.: Interaction in polysaccharide solution and gels. *Curr. Opin. Colloid Interface Sci.* 2003. vol. 8, pp. 396-400
17. Gascone, M. G.; Barbani, N.; Cristallini, C.; Giusti, P.; Lazzeri, L.: Bioartificial polymeric materials based on polysaccharides. *J. Biomaterial Sci Polym Ed.* 2001. vol. 12, pp. 267-281
18. Gong, Ch. Y.; Shi, S.; Wu, L.; et al: Biodegradable in situ gel-forming drug delivery system based on thermosensitive PCL-PEG-PCL hydrogel. Part 2: Sol-gel-sol transition and drug delivery behavior. *Acta Biomaterialia.* 2009. vol. 5, pp. 3358-3370
19. Holland, T. A.; Mikos, A. G.; *Biodegradable polymeric scaffolds. Improvements in bone tissue engineering through controlled drug delivery.* Adv. Biochem. Eng. Biotechnol. 2006. vol. 102, pp. 161-185
20. Behraves, E.; Yasko, A. W.; Engel, P. S.; Mikos, A. G.: Synthetic biodegradable polymers for orthopaedic applications. *Clin. orthop. Pelat. Res.* 1999. pp. S118-S129
21. Fisher, J. P.; Jo, S.; Mikos, A. G.; Reddi, A. H.: Thermoreversible hydrogel scaffolds for articular cartilage engineering. *J. Biomed, Mater. Res.* 2004. vol. 71, pp. 268-274
22. Laksmi, S.; Katti, D. S.; Laurencin, C. T.: Biodegradable polyphosphazenes for drug delivery applications. *Adv. Drug. Deliv. Rev.* 2003. vol. 55, pp. 467-482
23. Rizzi, S. C.; Heath, D. J.; Coombes, A. G.; Bock, N.; Textor, M.; Downes, S.: Biodegradable polymer/hydroxyapatite composites: surface analysis and initial attachment of human osteoblast. *J. Biomed Mater Res.* 2001. vol. 55, pp. 475-486
24. Huh, K., M.; Cho, Y., W.; Park, K.: PLGA-PEG Block Copolymers for Drug Formulations. *Drug Delivery Technology.* 2003, vol. 3, p. 1-10

25. George, J. H. S.: *Engineering of Fibrous Scaffolds for use in Regenerative Medicine*. Imperial college London. 2009, pp. 74–80. Dostupné z WWW: http://www.centropede.com/Thesis2009/JHGeorge_PhD_2009_forPDF_optimised.pdf
26. Lan, P.; Yhang, Y.; Gao, Q.; Shao, H; `Hu, X.: Studies on the Synthetic and Thermal Properties of Copoly(L-lactic/glycolic acid) by Direct Melt Polycondensation. *J of Applied Science*. 2003, vol. 92, pp. 2163–2168
27. Lee, J., Bae, Y. H., Sohn, Y. S., Jeong, B.: Thermogelling aqueous solutions of alternating multiblock copolymers of poly(L-lactic acid) and poly(ethylene glycol). *Biomacromolecules*. 2006, vol. 7, pp. 1729
28. Yokoyama, M.: *Crit. Rev. Ther. Drug Carrier Syst*. 1992. vol. 9, pp. 213–248
29. Gilbert, J. C.; Hadgraft, J.; Bye, A.; Brookes, L.: *Int. J. Pharm.* 1986. vol. 32, pp. 223–228
30. Jeong, B.; Kim, S. W.; Bae, Y. H.: Thermosensitive sol-gel reversible hydrogels. *Advanced Drug Delivery Reviews*. 2002, vol. 54, pp. 37–51
31. Loh, X. J.; Li, J.: *Biodegradation* thermosensitive copolymer hydrogel for drug delivery. *Expert Opinion Ther. Patents*. 2007, vol. 17, pp. 965–977
32. Bae, S. J.; Suh, J. M.; et al.: *Macromolecules*. 2005. vol. 38, pp. 5260–5265
33. Behraves, E.; Shung, A. K.; Jo, S.; Mikos, A. G.: *Biomacromolecules*. 2002. vol. 2, p. 153–158
34. Jeong, B.; Lee, M. K.; Gutowska, A.; An, Y., H.: Thermogelling Biodegradable Copolymer Aqueous Solutions for Injectable Protein delivery And Tissue Engineering. *Biomacromolecules*. 2002, vol. 3. pp. 865–868
35. Choi S.W.; Choi S. Y.; Jeong B.; Kim S. W.; Lee D. S: Thermoreversible Gelation of Poly(ethylene oxide) Biodegradable Polyester Block Copolymers. II, *Journal of Polymer Science: Part A: Polymer Chemistry*, 1999, 37, pp. 2207–2218
36. Lee, D. S.; Shim, M. S.; Kim, S. W. at al.: Novel Thermoreversible Gelation of Biodegradable PLGA-block-PEO-block-PLGA Triblock Copolymers in Aqueous Solution. *Macromol. Rapid Commun*. 2001, vol. 22, pp. 587–592
37. Yu, L.; Zhang, H.; Ding, J.: Effect of precipitate agents on temperature-responsive sol-gel transition of PLGA—PEG—PLGA copolymers in water. *Colloid Polym Sci*. 2010, vol. 288, pp. 1151–1159

38. Yu, L.; Zhang, Z.; Ding, J.: In vitro Degradation and Protein Release of Transparent and Opaque Physical Hydrogel of Block Copolymers at Body Temperature. *Macromolecular Research*. 2011, vol. 20, pp 234–243
39. Shim, M, S.; Lee, H., T.; et al: Poly(D, L-lactic acid-*co*-glycolic acid)-*b*-poly(ethylene glycol)-*b*-poly(D,L-lactic-*co*-glycolic acid) triblock copolymer and thermoreversible phase transition in water. *Journal of Biomedical Materials Research*, 2001, vol. 61 (2), pp. 188–196
40. Yu, L.; Zhang, Z.; Ding, J.: Influence of LA and GA Sequence in the PLGA Block on the Properties of Termogelling PLGA—PEG—PLGA Block Copolymers. *Biomacromolecules*. 2011, vol. 12, pp. 1290–1297
41. Huang, S. J., Edelman, P. G., Han, Y. K.: Synthesis and characterization of crosslinked polymers for biomedical composites. *J. Macromol. Sci. Chem. A* 25, 1988, vol. 8, pp. 47
42. Turunen, M. P. K., Korhonen, H., Tuominen, J., Seppälä, J. V.: Synthesis, characterization and crosslinking of functional star-shaped poly(ϵ -caprolactone). *Polymer. International*. 2001, vol. 51, pp. 92
43. Han, D. K., Hubbell, J. A., Surface characteristics and biocompatibility of lactide-based poly(ethylene glycol) scaffolds for tissue engineering. *Macromolecules*. 1997, vol. 30, pp. 6077
44. Helminen, A., Korhonen, H., Seppälä, J. V.: Synthesis of poly(ester-anhydride)s based on poly(ϵ -caprolactone) prepolymer. *J. Appl. Polym. Sci.* 2001. vol. 81, pp. 176–185
45. Tian, D., Dubois, Ph., Jérôme, R.: *J. Polym. Sci. A* 35, 2295 (1997). Biodegradable and biocompatible inorganic–organic hybrid materials. I. Synthesis and characterization. *Journal of Polymer Science Part A: Polymer Chemistry* .1997, vol .35, pp. 2295–2309
46. Korhonen, H., Helminen, A., Seppälä, J. V.: Biodegradable crosslinked polymers based on triethoxysilane terminated polylactide oligomers. *Polymer*. 2001, vol. 42, pp. 3345
47. Michlovská, L.; Vojtová, L.; Mravcová, L.; Hermanová, S.; Kučerík, J.; Jančář, J.: Functionalization Conditions of PLGA—PEG—PLGA Copolymer with Itaconic Anhydride. *Macromol. Symp.* 2012, vol. 295, pp. 119–124.
48. Reddy, C. S. K.; Singh, R. P.: *Enhanced production of itaconic acid from corn strach and market refuse fruits by genetically manipulated Aspergillus terreus SKR10*. *Bioresource Technology*. 2002, 8, p. 69–71.
49. Adler, J., Wang, S-F., Lardy, H. A. (1957). The Metabolism of Itaconic Acid by Liver Mitochondria. *J. Biol. Chem.*. 1957, vol. 229, pp. 865–879

50. Coombes, A. G.; Meikle, M.C.; *Resorbable* synthetic polymers as replacements for bone graft. *Clin Mater.* 1994. vol. 17, pp. 35–67
51. Laurencin, C. T.; Attawia, M.; Borden, M. D.: Advancements in tissue engineered bone substitutes. *Curr Opin Orthop.* 1995, vol. 10, pp. 445–451
52. de Boer, H. H.: The history of bone grafts. *Clin Orthop Relat Res.* 1988, vol. 226, pp. 292–298
53. Vacanti, C. A.; Kim, W.; Upton, J.; Vacanti, M. P.; Mooney, D.; Schloo, B.; et al: *Tissue-engineering growth of bone and cartilage.* Transport Proc. 1993. vol. 25, pp. 1019–1021
54. Coombes, A. G. A.; Meikle, M. C.: *Resorbable Synthetic Polymers as Replacements for Bone Graft.* Clinical Materials. 1994, vol. 17, pp. 35–67
55. Welch, R. D.; Jones, A. L.; Bucholz, R. W.; Reinert, C. M.; Tjia, J. S.; Pierce, W. A.; Wozney, J. M.; Li, X. J.: Effect of recombinant human bone morphogenetic protein-2 on fracture healing in a goat tibial fracture model. *J Bone Miner Res.* 1998. vol. 13, pp. 1498–1490
56. Swetha, M.; Sahithi, K.; et al: Biocomposites containing natural polymers and hydroxyapatite for bone tissue engineering. *International Journal of Biological Macromolecules.* 2010, vol. 47, pp.1–4
57. Dorozhkin, S. V.: Bioceramics of calcium orthophosphates. *Biomaterials.* 2010, vol. 31, pp. 1465–1485
58. Fu, Q.; Tomsia, A. P.; Saiz, E. Bioactive Glass Scaffolds for Bone Regeneration. *ALSNews.* 2011, vol. 324. Dostupné z WWW: < <http://www-als.lbl.gov/index.php/science-highlights/science-highlights/588-bioactive-glass-scaffold-for-bone-regeneration.html>>.
59. Vitale-Brovarone, C.; Verné, E.; et al: Development of glass-ceramics scaffolds for bone tissue engineering: Characterization, proliferation of human osteoblasts and nodule formation. *Acta Biomaterials.* 2003, vol. 3. pp. 199–208
60. Niinomi, M.: Recent research and development in titanium alloys for medical applications and healthcare goods. *Science and Technology of Advanced Materials.* 2003, vol. 4, pp. 445–454
61. Armentano, I.; Dottori, M.; Fortunatti, E.; Mattioli, S.; Kenny, J.M.: Biodegradable polymer matrix nanocomposites for tissue engineering: A review. *Polymer Degradation and Stability.* 2010, vol. 95, pp. 2126–2146

62. Kokubo, T.; Takadama, H.: How useful is SBF in predicting in vivo bone bioactivity. *Biomaterials*. 2006, vol. 27, pp. 2907–2915
63. Hench, L. L.: Bioceramics. *J Am Ceram Soc*. 1998, vol. 81, pp. 1705–1728
64. Davies, J. E.: *Bone Engineering. En Squared Incorporated*, 1999. Toronto, Canada, chapter 13, pp. 152–160.
65. Ducheyn, P.; Qiu, Q.: Bioactive ceramics: the effect of surface reactivity on bone formation and bone cell function. *Biomaterials*. 1999, vol. 20, pp. 2287–2303.
66. Vallet-Regí, M.: Evolution of bioceramics within the field of biomaterials. *C. R. Chimie*. 2010, vol. 13, pp. 174–185
67. De Aza, P.N.; De Aza, A.H.; Pena, P.; De Aza S.: Bioactive glass and glass-ceramics. *Boletín de la Sociedad Española de Cerámica y Vidrio*. 2007, vol. 26, pp. 45–55
68. Kokubo, T.: Bioactive glass-ceramics: properties and applications. *Biomaterials*. 1991, vol. 12, pp. 155–163
69. *Cerabone* [online]. 2011 [cit. 2011-12-06]. Dostupné z WWW: <http://www.aap.de/en/Produkte/Orthobiologie/Knochenersatz/Cerabone/index_html>.
70. Urban, K.; Stehlík, J.: Initial clinical experience with BAS O, a bioactive glass-ceramic material. *Acta Chir Orthop Traumatol Cech*. 1993, vol. 60, p. 40–46.
71. Staiger, M. P.; Pietak, A., M.; Huadmai, J.; Dias, G.: Magnesium and its alloys as orthopedic biomaterials: A review. *Biomaterials*. 2006, vol. 27, pp. 1728–1734
72. Sudhakar, K. V.: Investigation of failure mechanism in vitallium 2000 implant. *Engineering Failure Analysis*. 2005, vol 12, pp. 257–262.
73. Meticoš-Huković, M.; Pilić, Z.; Babić, R.; Omanović, D.: Influence of alloying elements on the corrosion stability of CoCrMo implant alloy in Hank's solution. *Acta Biomaterialia*. 2006, vol. 2, pp. 693–700.
74. Huang, H. H.: Surface characterization of passive film on NiCr based dental casting alloys. *Biomaterials*. 2003, vol. 24, pp. 1575–1582.
75. Li, C.; Zheng, Y. F.: The electrochemical behavior of a Ti₅₀Ni₄₇Fe₃ shape memory alloy. *Materials Letters*. 2006, vol. 60, pp. 1646–1650.
76. Nagels, J.; Stokdijk, M.; Rozing, P. M.: Stress shielding and bone resorption in shoulder arthroplasty. *J Shoulder Elbow Surg*. 2003, vol. 12, pp. 35–39

77. Harlan, C, et al. Metal-on-Metal Hybrid Surface Arthroplasty: Two to Six-Year Follow-up Study. *The Journal of Bone & Joint Surgery*. 2004, vol. 86, p. 28–39
78. *Azom* [online]. 2008 [cit. 2011-12-08]. Dostupné z WWW: <<http://www.azom.com/article.aspx?ArticleID=4264>>.
79. *Glass Effect* [online]. 2010 [cit. 2011-12-08]. Dostupné z WWW: <<http://glasseffects.wordpress.com/page/4/>>.
80. *Dental Tribune* [online]. 2010 [cit. 2011-12-08]. Dostupné z WWW: <<http://www.dental-tribune.com/articles/content/id/1321>>.
81. Gao, Y.; Cao, W., L.; Wang, X., Y.: Characterization and osteoblast-like cell compatibility of porous scaffolds: bovine hydroxyapatite and novel hydroxyapatite artificial bone. *Journal of Material Science: Material in Medicine*. 2006, vol 17, pp. 815–823
82. Ruksudjarit, A; Pengpat, K.; Rujijanagul, G.; Synthesis and characterization of nanocrystalline hydroxyapatite from natural bovine bone. *Current Applied Physics*. 2008, vol. 8, pp. 270–272
83. Ono, I.; Tateshita, T.; Nakajima, T.: Evaluation of a high density polyethylene fixing system for hydroxyapatite ceramic implants. *Biomaterials*. 2000, vol. 21, pp. 143–151
84. Sinha, A.; Mishra, T.; Ravishankar, N.: Polymer assisted hydroxyapatite microspheres suitable for biomedical application. *The Journal of Material Science: Materials in Medicine*, 2008. vol. 19, pp. 2009–2013
85. Lusquinos, F.; De Carlos, A.; Pou, J.; Aries, J., L.; et al.: Calcium phosphate coatings obtained by Nd:YAG laser cladding: Physicochemical and biologic properties. *Journal of Biomedical Materials Research Part A.*, 2003, vol. 23. pp. 630–637
86. Haiying, Y.; Matthew, H., W.; Wooley, P., H.; Yang, S.-Y.: Biocompatibility of Poly- ϵ -caprolactone-hydroxyapatite composite on mouse bone marrow-derived osteoblasts and endothelial cells. *Journal of Biomedical Materials Research*. 2007, vol. 86, pp. 540
87. Katanec, D.; Pavelić, B.; Ivasović, Z.: Efficiency of Polylactide/Polyglycolide Copolymers Bone Replacements in Bone defects Healing Measured by Densitometry. *Coll. Antropol.* 2004, vo. 28, pp. 331–336
88. Lee, J., B.; Lee, S., H; et al.: PLGA scaffold incorporated with hydroxyapatite for cartilage regeneration. *Surface & Coating Technology*. 2008, vol. 202, pp. 5757–5761
89. Lee, J., B.; Kim, S., E., et al.: In vitro Characterization of Nanofibrous PLGA/Gelatin/Hydroxyapatite Composite for Bone Tissue Engineering. *Macromolecular Research*. 2010, vol. 18, pp. 1195–1202

90. Santos, C.; Luklinska, Y. B.; Clarke, R. L.; Davy, R. L.: Hydroxyapatite as filler for dental composites materials: evaluation of mechanical properties and in vitro bioactivity of composites. *Journal of Materials Science, Materials in Medicine*. 2001. vol. 12, pp. 565–573
91. Xiangnan, L.; Xiaoming, CH.; Shipu, L.; Zhiming, P.: Synthesis and Charakterization of Core-shell Hydroxyapatite/Chitosan Biocomposite Nanospheres. *Journal of Wuhan University of Technology-Mater*. 2010. vol. 25, pp. 252–256
92. Barnes, H.A.: *A Handbook of Elementary Rheology*. Institute of Non-Newtonian Fluid Mechanics, Aberystwyth. 2000
93. Teraoka, I.: *Polymer solutions: An Introduction to Pysical Properties*. Polytechnic University, New York. 2002. ISBN 0-471-38923-3
94. Chhabra, R., P.; Richardson, J., F.: *Engineering application*. Non-Newtonian flow and applied Rheology. Second edition 2008, pp. 5–14
95. [Http://translate.google.cz/translate?hl=cs&sl=en&tl=cs&u=http%3A%2F%2Fwww.research-equipment.com%2Fviscosity%2520chart.html&anno=2](http://translate.google.cz/translate?hl=cs&sl=en&tl=cs&u=http%3A%2F%2Fwww.research-equipment.com%2Fviscosity%2520chart.html&anno=2) [online]. 2008 [cit. 2011-07-19].
96. Sperling, L.H.: *Introduction to Physical Polymer Science*. Lehigh university. 2006, 4th edition
97. TA INSTRUMENT. *Rheology Theory and Applications Course*. 2008. vyd. USA.
98. Wang, Y-x.; TAN, Y-b.; Huang, X-l.: *Rheological properties of novel thermo-responsive polycarbonates aqueous solutions*. J. Cent. South Univ. Technol. 2008, vol. 15, pp. 102–106
99. <http://pediatriccardiology.uchicago.edu/pp/abnl%20rhythm%20for%20parents%20body.htm>
100. Winter, H. H.; Chambon, F.: Analysis of linear Viscoelasticity a Crosslinking Polymer at the Gel Point. *Journal of Rheology*. 198, vol. 13. pp. 367-382
101. Zentner, G. M.; et al: Biodegradable block copolymer for drug delivery of proteins and water-insoluble drugs. *Journal of Controlled Release*. 2001, vol. 72, pp. 203–215.

7 APPENDICES

7.1 The List of Pictures

Fig. 1 Natural polymers.....	9
Fig. 2 Schematic presentation of block copolymer structure (a) A-B diblock, (b) A-B-A triblock, (c) B-A-B triblock, (d) alternating multiblock, (e) multi-armed structure, (f) star-shape block.	11
Fig. 3 Formula of ABA-type triblock copolymer PLGA—PEG—PLGA.	12
Fig. 4 A typical phase diagram of ABA-type PLGA-block-PEO-block-PLGA triblock copolymer in water [36].	13
Fig. 5 Micellar gelation mechanisms for ABA-type triblock copolymer in aqueous solution.	14
Fig. 6 Chemical structure of ITA/PLGA—PEG—PLGA/ITA, where $M_{n(PEG)} = 1\,500\text{ g}\cdot\text{mol}^{-1}$	15
Fig. 7 Classification of non-resorbable, partially and fully resorbable composites [10].....	16
Fig. 8 Skeletal system structure of a human bone [6].	17
Fig. 9 (a) Metal prosthesis [77], (b) ceramic orthopaedic implants [78], (c) 3-dimensional biomass-scaffold [79], (d) glass-ceramic crown used in dental applications [80].....	19
Fig. 10 Hydroxyapatite.....	19
Fig. 11 Flow curves for different types of fluids.....	22
Fig. 12 The most commonly used geometry in dynamic rheological analysis.	23
Fig. 13 Increasing value of sinusoidal amplitude (strain or stress).	23
Fig. 14 Frequency sweep.....	24
Fig. 15 Typical Maxwellian behavior in oscillatory testing, with the crossover point indicated [93].....	25
Fig. 16 Evaluation of G^* with the increasing value of shear rate.....	25
Fig. 17 Evaluation of the storage modulus G' and the loss modulus G'' of a crosslinking polymers.	26
Fig. 18 Thermoblock used for test tube inverting method.	29
Fig. 19 (a) adding cold polymer solution (b) working position (c) lid was used to prevent evaporation of the sample.....	30
Fig. 20 SEM micrographs of the HAp powder.	32
Fig. 21 Particle size analysis of HAp powder.	33
Fig. 22 Evaluation of gel with increasing temperature for PLGA—PEG—PLGA triblock copolymer ($c = 22\text{ wt}\%$).	34
Fig. 23 Phase transition diagram of PLGA—PEG—PLGA triblock copolymer (sample A).....	35
Fig. 24 Phase transition diagram of PLGA—PEG—PLGA triblock copolymer (sample A1).....	35

Fig. 25 Phase transition diagram of ITA/PLGA–PEG–PLGA/ITA (sample B).....	36
Fig. 26 Dynamic moduli of sample A1 (c = 22 wt %) at a fixed frequency of 1.0 rad·s ⁻¹ and temperature 37 °C.	37
Fig. 27 Dynamic moduli (polymer concentration c = 22 wt %) at a fixed frequency of 1.0 rad·s ⁻¹ and temperature 37 °C for sample with HAp	38
Fig. 28 Dynamic moduli of sample A1 (c = 22 wt %) at 37 °C and fixed oscillatory stress at 0.4 Pa.	39
Fig. 29 Dynamic moduli of sample A1 (c = 22 wt %) with 20 % of HAp at 37 °C and fixed oscillatory stress at 0.4 Pa.	39
Fig. 31 Evaluation of elastic modulus (G') of different concentration of PLGA—PEG— PLGA solution in ultrapure water – sample A1 (PLGA/PEG = 2.5) and sample A (PLGA/PEG = 2.0).	41
Fig. 32 Rheological measurement of sample A water solution (c = 24 wt %), where (1) is sol-gel transition and (2) is gel-suspension transition	41
Fig. 33 Thermogelling behaviors by TTIM and rheology of different concentration of PLGA—PEG—PLGA solution in ultrapure water – sample A (PLGA/PEG = 2.0)... ..	42
Fig. 34 Elastic modulus of ITA/PLGA—PEG—PLGA/ITA (sample B) at different concentration in ultrapure water.	43
Fig. 35 Thermogelling behavior by TTIM and rheology of different concentration of ITA/PLGA—PEG—PLG/ITA solution in ultrapure water – sample B (PLGA/PEG = 2.0).	44
Fig. 36 Evaluation of elastic modulus (G') of different concentration of PLGA—PEG— PLGA solution in ultra pure water – sample A (PLGA/PEG = 2.0) and sample B (PLGA/PEG = 2.5).	45
Fig. 37 Elastic modulus (G') as a function of temperature and adding amount of HAp- powder, c = 10 wt % of PLGA—PEG—PLGA in ultrapure water.....	46
Fig. 38 Dependence of elastic moduli on adding amount of HAp-powder.....	47
Fig. 39 Influence of added amount of HAp (wt%) on the temperature of maximum gel stiffness (G' _{max}).	48

7.2 The List of Tables

Table 1: Physical properties of biodegradable polymers	10
Table 2: Mechanical properties of hard and soft tissue	16
Table 3: Newtonian and Non-Newtonian fluid.....	22
Table 4: Chemical properties of prepared copolymers	31
Table 5: Comparison of cross-points noticed by TTIM and rheological analysis	42
Table 6: Viscoelastic properties of unmodified and ITA modified PLGA—PEG—PLGA copolymer, c = 22 wt %	45
Table 7: Changing of G' (Pa) and pH with adding amount of HAp	46

7.3 The List of Abbreviations

BIS-GMA	bis-phenol A glycidyl methacrylate
CF	carbon fiber
CGC	critical gel concentration
CGT	critical gelation temperature
CMC	critical micelle concentration
CS	chitosan
DPH	1,6-diphenyl-1,3,5-hexa-triene
GF	glass fiber
HAp (HA)	hydroxyapatite
HDPE	high-density poly(ethylene)
¹ H NMR	proton nuclear magnetic resonance
HFIP	hexafluoroisopropanol
ITA	itaconic anhydride
KF	kevlar fiber
γ-MPS	methacryloxypropyltrimethoxy-silane
PBS	phosphate buffer saline
PBT	poly(hydroxybutyrate)
PC	poly(carbonate)
PCL	poly(ε-caprolactone)
PDMS	polydimethylsiloxane
PE	poly(ethylene)
PEEK	poly(etheretherketone)
PEG	poly(ethylene glycol)
PET	poly(ethyleneterephthalate)
PHEMA	poly(hydroxyethyl methacrylate)
PGA	poly(glycolic acid)
PLA	poly(lactic acid)
PLDLLA	poly(L-D,L-lactide)
PLLA	poly(L-lactic acid)
PLGA	poly(D,L-lactic acid-co-glycolic acid)
PMA	poly(methacrylate)
PMMA	poly(methylmethacrylate)
PPO	poly(propylene oxide)
PP	poly(propylene)
PS	poly(styrene)
PTFE	poly(tetrafluoroethylene)
PU	poly(urethane)
ROP	ring-opening polymerization
TTIM	test tube inverting method

7.4 The List of Symbols

G'	shear storage modulus
G''	shear loss modulus
G^*	complex modulus
$\tan \delta$	loss tangent
M_n	number-average molecular weight
M_w	mass-average molecular weight
M_w/M_n	polydispersity index
T_g	glass transition temperature ($^{\circ}\text{C}$)
T_m	melting point ($^{\circ}\text{C}$)
γ	strain
γ_0	strain oscillatory amplitude
$\dot{\gamma}$	shear rate (s^{-1})
δ	phase angle
η^*	complex viscosity ($\text{Pa}\cdot\text{s}$)
σ	stress (Pa)
τ	shear stress (Pa)
τ_0	stress oscillatory amplitude (Pa)
ω	angular frequency ($\text{rad}\cdot\text{s}^{-1}$)
t	time (s)